

Review

# Glycerol Production and Transformation: A Critical Review with Particular Emphasis on Glycerol Reforming Reaction for Producing Hydrogen in Conventional and Membrane Reactors

Giuseppe Bagnato <sup>1</sup>, Adolfo Iulianelli <sup>2,\*</sup>, Aimaro Sanna <sup>1</sup> and Angelo Basile <sup>2,\*</sup>

<sup>1</sup> School of Engineering & Physical Sciences, Heriot-Watt University, Edinburgh EH14 4AS, UK; gb17@hw.ac.uk (G.B.); a.sanna@hw.ac.uk (A.S.)

<sup>2</sup> Institute on Membrane Technology of the Italian National Research Council (ITM-CNR), c/o University of Calabria, via P. Bucci Cubo 17/C, 87036 Rende (CS), Italy

\* Correspondence: a.iulianelli@itm.cnr.it (A.I.); a.basile@itm.cnr.it (A.B.); Tel.: +39-0984-492011 (A.I.); +39-0984-492013 (A.B.)

Academic Editor: Edward Gobina

Received: 12 January 2017; Accepted: 17 March 2017; Published: 23 March 2017

**Abstract:** Glycerol represents an emerging renewable bio-derived feedstock, which could be used as a source for producing hydrogen through steam reforming reaction. In this review, the state-of-the-art about glycerol production processes is reviewed, with particular focus on glycerol reforming reactions and on the main catalysts under development. Furthermore, the use of membrane catalytic reactors instead of conventional reactors for steam reforming is discussed. Finally, the review describes the utilization of the Pd-based membrane reactor technology, pointing out the ability of these alternative fuel processors to simultaneously extract high purity hydrogen and enhance the whole performances of the reaction system in terms of glycerol conversion and hydrogen yield.

**Keywords:** glycerol production; glycerol steam reforming; conventional reactor; membrane reactor; hydrogen

## 1. Introduction

The need for replacing fossil fuels is driving the development of renewable fuels such as biodiesel. In the period 2000–2012, biodiesel production increased from 15 to 430 thousand barrels (Figure 1) [1–3]. In the process of producing biodiesel from the transesterification of vegetable oils, glycerol (propane-1,2,3-triol) is produced as by-product. Typically, the production of 100 kg of biodiesel yields approximately 10 kg of glycerol, with purity of around 50%–55% [1].

The increased production of bio-diesel resulted in a significant fall of glycerol prices from 2000 to 2010 in the European Union (EU) and USA, as can be seen in Figure 2. In particular, the price dramatically decreased from about 3200 \$/ton in EU and 2000 \$/ton in USA to under 500 \$/ton and 600 \$/ton, respectively. This was mainly due to a new demand in developing countries as China, India, Russia and Latin American countries, where the glycerol was utilized as raw material in the personal care, pharmaceuticals and food and beverage sectors [4–6].

Currently, glycerol is mainly used as an intermediate chemical for the production of a variety of products [7], such as cosmetics, food, pharmaceuticals, etc., as represented in Figure 3.

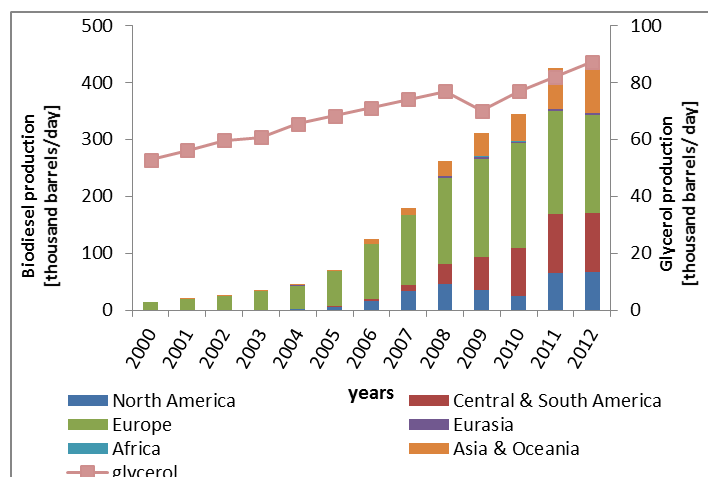


Figure 1. Biodiesel and glycerol production vs. years.

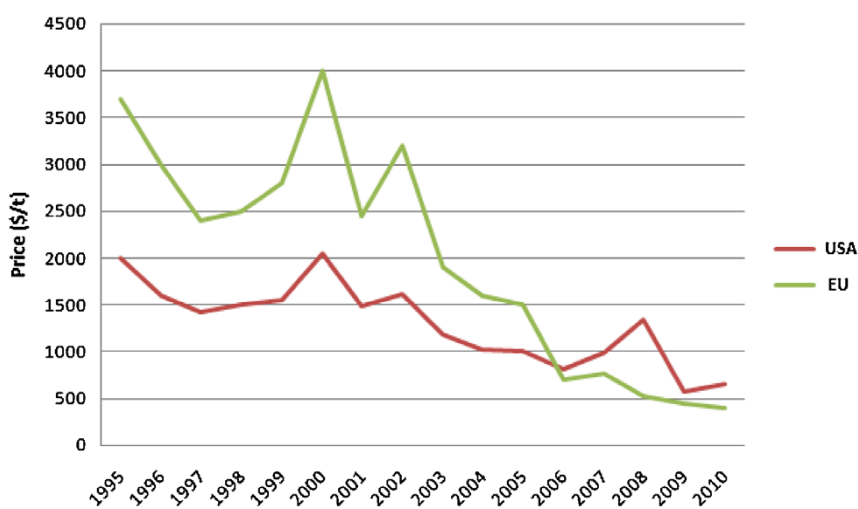


Figure 2. Glycerol price trend in USA and UE. With permission of reprint by Wiley from [1].

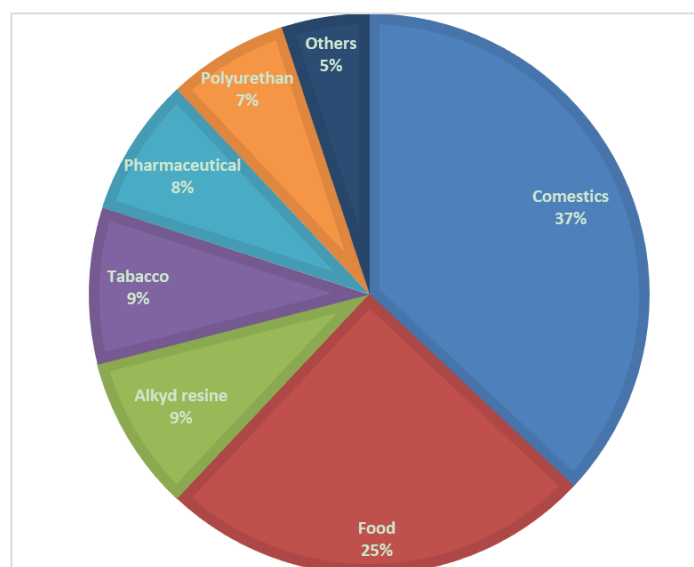


Figure 3. Percentage distribution of the main glycerol applications found in the open literature.

### 1.1. Glycerol Production

Glycerol can be produced by using different processes and feedstocks. For example, it can be obtained by propylene synthesis via several pathways [8], by hydrolysis of oil or by transesterification of fatty acids/oils. Nevertheless, glycerol production can be also carried out by fermentation with yeast such as *saccharomyces cerevisiae*, *candida*, bacteria such as *Bacillus subtilis* and algae such as *dunaliella tertiolecta* [9].

#### 1.1.1. Glycerol via Propylene

As stated before, several pathways can be used for producing glycerol by propylene [3,10] and Figure 4 sketches two of the principal pathways, which involve the use of O<sub>2</sub> or Cl<sub>2</sub>.

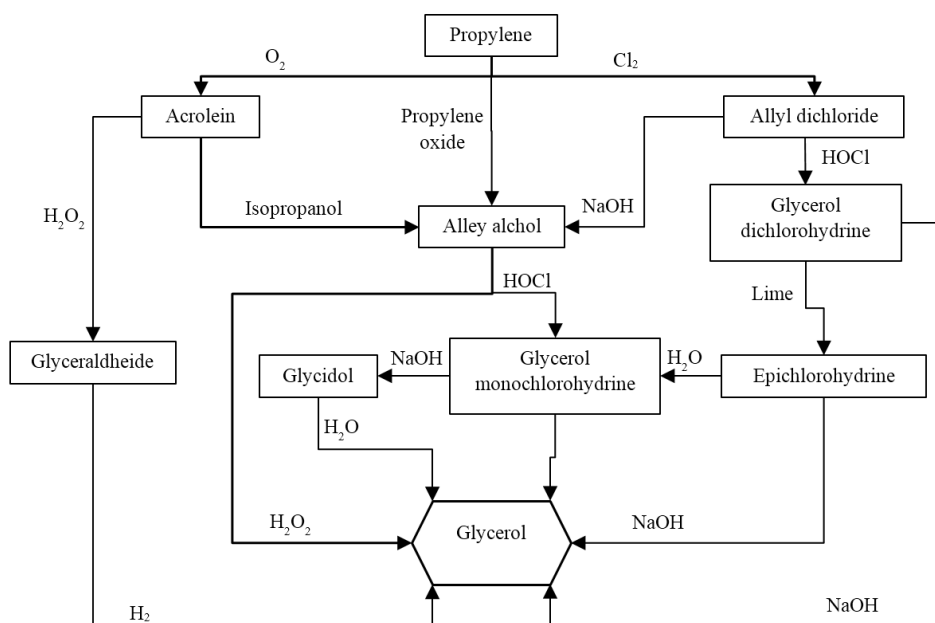


Figure 4. Glycerol production via propylene utilization.

In the propylene chlorination (Figure 5), allyl chloride is produced at 510 °C in presence of hypochlorous acid at 38 °C. The allyl chloride reacts to produce glycerine dichlorohydrine. Afterwards, glycerine dichlorohydrine is hydrolysed by caustic soda in a 6% Na<sub>2</sub>CO<sub>3</sub> solution at 96 °C or directly to glycerine, taking off the epichlorohydrine as an overhead in a stripping column. At the end, the epichlorohydrine is hydrated to glycerine with caustic soda [3] and the process makes possible final glycerol yield of about 90%.

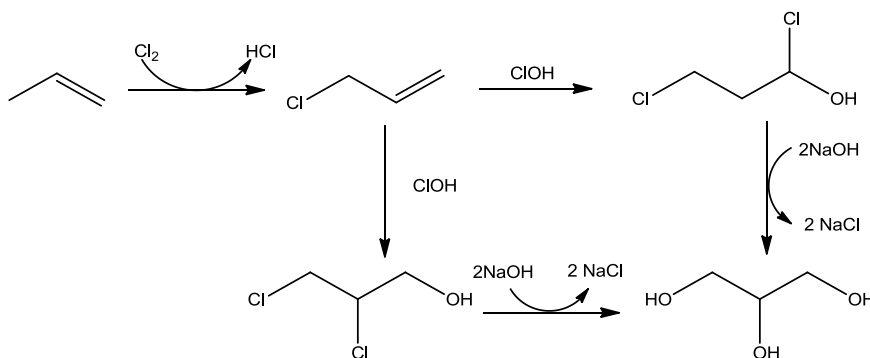
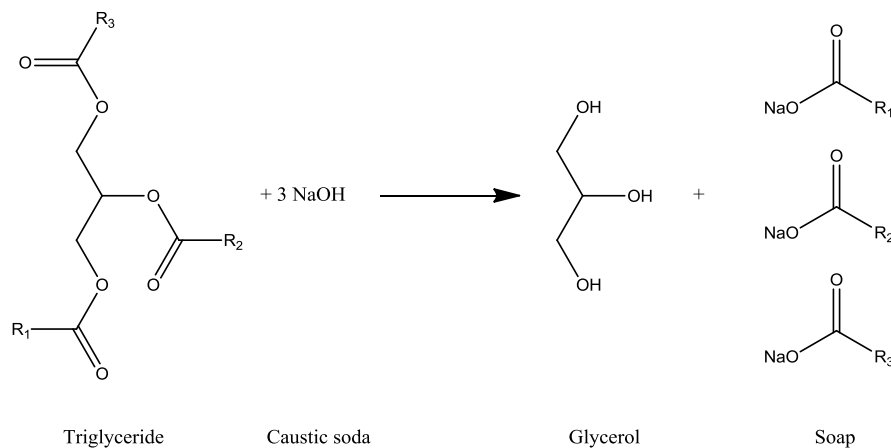


Figure 5. Scheme of the propylene chlorination process.

### 1.1.2. Hydrolysis of Oil

The hydrolysis is a process known since 2800 B.C. and the first industrial plant was built up in 1860 [11]. This reaction takes place between triglyceride and alkaline hydroxide (caustic soda) producing glycerol and soap [12] (Figure 6).



**Figure 6.** Hydrolysis reaction for glycerol production.

### 1.1.3. Transesterification of Oil

The transesterification reaction of the beaver oil with ethanol to produce glycerol was conducted in 1864 by Rochieder [5,13]. Figure 7 represents the schematic of the reaction, where methyl-esters from triglyceride (oils) and methanol (alcohol) react to produce glycerol and fatty esters (or biodiesel) [10,14,15].

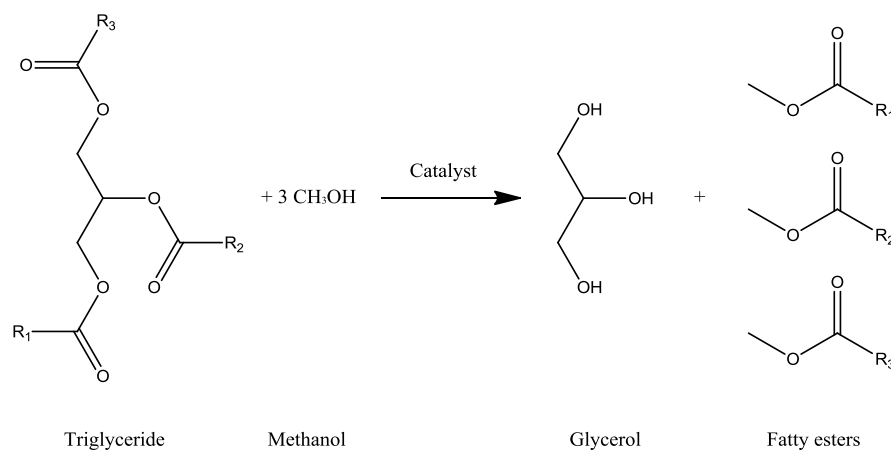


**Figure 7.** Transesterification reaction for glycerol production.

Homogeneous and heterogeneous catalysis can be used to produce bio-diesel and thereby for glycerol production. The process using homogeneous catalysts (in particular, sodium hydroxide or sodium methylate) [13,16] is shown in Figure 8. The first process step involves the reaction between vegetable oils and methanol in presence of the catalyst; subsequently, the glycerol separation from the mixture of products by settler unit takes place. The remnants flow is sent to a unit for the removal of the catalytic component with mineral acids, producing two streams: a glycerol recovery unit and an evaporator, which separates biodiesel from the other products. The glycerol purification unit has three output streams: the first containing 80%–95% of glycerol, the 2nd consisting of water, dissolved salts and unreacted methanol (which is recycled back to the reactor) and the 3rd stream that contains fatty ester [15].

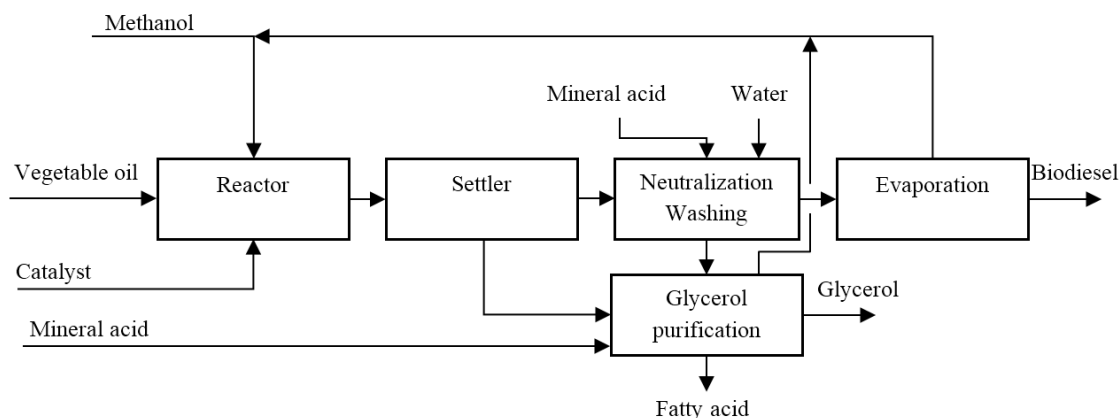


Figure 8. Biodiesel production plant based on homogenous catalyst utilization.

The block diagram of triglycerides trans-esterification with heterogeneous catalysts (mainly aluminium and zinc oxides) is reported in Figure 9. To increase the vegetable oil conversion, the process foresees two reaction steps; the first reactor is fed by vegetable oil and methanol. The product stream passes through a heat exchanger to evaporate part of the unreacted methanol, while the remaining stream is sent to a decanter to separate polar (largely glycerol) and non-polar (most vegetable oil and biodiesel) components. In the second reactor, the non-polar stream is reacted for the 2nd time to increase the production of biodiesel and recover the methanol. The product stream passes through the heat exchanger, which removes the entire unreacted methanol, while the decanter separates the biodiesel from polar components. The polar streams of both the first and second polar decanters are sent to another heat exchanger for recovering the remaining methanol present in the mixture, while the residual part is sent into a final decanter for the separation of vegetable oil and unreacted glycerol.

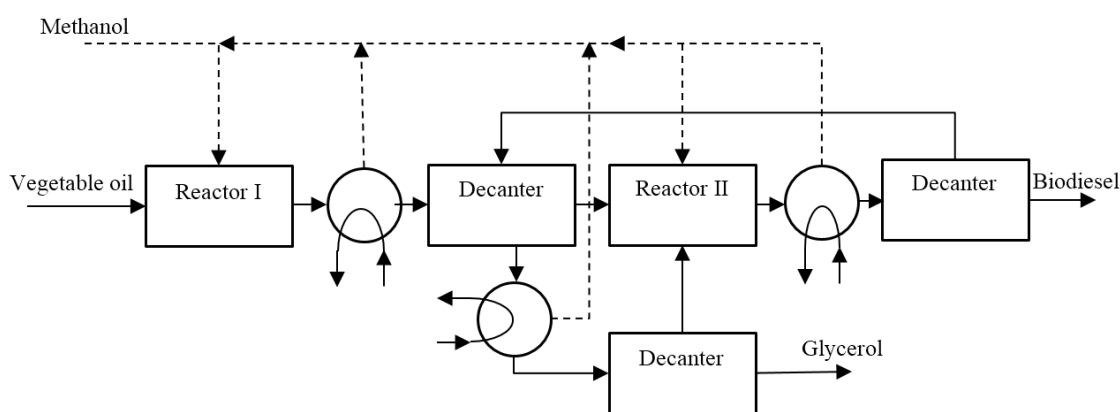


Figure 9. Biodiesel production plant scheme based on heterogeneous catalyst.

The process of the transesterification reaction through supercritical fluids has been largely studied, even though it is not yet industrialised. One or two reaction steps are possible: in single-step supercritical fluid transesterification, the reaction takes place only after the heating up of reactants to their critical temperature and pressure with triglycerides [17,18]; in two-step subcritical-supercritical fluid transesterification, triglycerides are firstly converted to free fatty acids and by-products, in the hydrolysis reaction. Subsequently, the obtained free fatty acids undergo esterification reaction and produce fatty acid methyl esters in supercritical fluid reaction [19,20].

Depending on the process and feedstock, the glycerol stream is characterized by several compositions; therefore, its characteristics can be identified looking at the different types of feedstocks and reactions utilized during the production process [21–28], as summarized in Table 1.

**Table 1.** Characteristic of different glycerol streams depending on initial feedstocks and production reactions (Adapted from [28]).

Feedstock	Glycerol (w/w)	Methanol (w/w)	Soap (w/w)	MONG (w/w)	Ref.
Waste of palm oil	87.1%	–	–	5.5%	[21]
Jatropha oil	18.0%–22.0%	14.5%	29.0%	11.0%–21.0%	[22]
Soybean oil	63.0%	6.2%	–	–	[23]
Soybean oil	22.9%	10.9%	26.2%	23.5%	[23]
Soybean oil	33.3%	12.6%	26.1%	22.3%	[23]
Waste vegetable oil	27.8%	8.6%	20.5%	38.8%	[23]
Palm oil	80.5%	0.5%	–	<2.0%	[24]
Seed oils	62.5%–76.6%	–	–	–	[25]
Used frying oil	85.3%	–	–	14.7%	[26]

Tan et al. [25] reviewed most of the advantages and disadvantages of the various techniques of transesterification, which we updated in this work by adding the transesterification reaction whit supercritical fluid (Table 2).

**Table 2.** Advantages and disadvantages of biodiesel and glycerol production by oil transesterification (Adapted from [25]).

Catalysts Group	Type of Catalyst	Advantage	Disadvantage
Homogeneous base catalyst	NaOH KOH	Very fast reaction rate The reaction can occur at mild reaction condition and less energy intensive High conversion can be achieved These catalysts are widely available and economical	The usage limits for oil with less than 0.5 wt % FFA Soap will be formed if the FFA content in the oil is more than 2 wt % Excessive soap formation will reduce the biodiesel yield and cause the problem during the product purification
Heterogeneous base catalyst	CaO MgO	Relatively faster reaction rate than acid catalysed transesterification The reaction can occur at mild reaction condition and less energy intensive Easy separation of catalyst from product High possibility to reuse and regenerate the catalyst	Sensitive to FFA content in the oil due to its basicity property Soap will be formed if the FFA content in the oil is more than 2 wt % Excessive soap formation will decrease the biodiesel yield and cause the problem during product purification Leaching of catalyst active sites may result to product contamination
Homogeneous acid catalyst	H <sub>2</sub> SO <sub>4</sub> HCl	Insensitive to FFA content and water content in the oil Preferred-method if low-grade oil is used Esterification and transesterification can occur simultaneously The reaction can occur at mild reaction condition and less energy intensive More economical than base catalysed process	Very slow reaction rate Required high reaction temperature and high molar ratio of alcohol to oil Corrosive catalyst such as H <sub>2</sub> SO <sub>4</sub> used can lead to corrosion on reactor and pipelines Separation of catalyst from product is problematic
Heterogeneous acid catalyst	ZrO <sub>2</sub> TiO <sub>2</sub> SnO <sub>2</sub> Zeolite	Insensitive to FFA content and water content in the oil Preferred-method if low-grade oil is used Esterification and transesterification occur simultaneously Eliminate the washing step of biodiesel Easy separation of catalyst from product High possibility to reuse and regenerate the catalyst Reduce corrosion problem	Complicated catalyst synthesis procedures lead to higher cost Required high reaction temperature, high alcohol to oil molar ratio and long reaction time are required Energy intensive Leaching of catalyst active sites may result to product contamination
Enzyme	Mucor miehei (Lipozym IM60) C. antarctica (Novozym435) Bacillus subtilis	Insensitive to FFA and water content in the oil Preferred-method flow-grade oil is used Transesterification can be carried out at a low reaction temperature, even lower than homogeneous base catalyst Only simple purification step is required	Very slow reaction rate, even slower than acid catalyzed transesterification High cost Sensitivity to alcohol, typically methanol that can deactivate the enzyme
Supercritical fluid	Noncatalytic	Potential and value of by-products. triacetin and glycerol carbonate were produced in supercritical methyl acetate and dimethyl carbonate technology, respectively High process flexibility of feedstock conditions. Impurities presence of water and FFA do not give any detrimental effects to the product yield	High energy consumption

## 1.2. Glycerol Applications

Glycerol can be converted into other compounds with high added value, such as butanol, 1,3-propanediol, 2,3-butanediol, citric acid, lipid, poly(hydroxyalkanoates), acrolein, monoglycerides, etc., via oxidation, reduction, esterification, etc. [27–29], by conventional (Table 3) or fermentation process (Table 4).

**Table 3.** Products coming from glycerol conversion by conventional process with related operating conditions.

Reaction Type	Product	Reactant	Catalyst	<i>p</i> (bar)	<i>T</i> (°C)	Ref.
Glycerol oxidation	Dihydroxyacetone	O <sub>2</sub>	Pd–Ag/C	3	80	[30]
		O <sub>2</sub>	Pt/MWCNT	–	60	[31]
		O <sub>2</sub>	Au/MWCNT	3	60	[32]
		O <sub>2</sub>	Pt/SiO <sub>2</sub>	1	100	[33]
	Glyceraldehyde	O <sub>2</sub>	Pt/MCN	3	40	[34]
		O <sub>2</sub>	Pt/SiO <sub>2</sub>	1	100	[33]
	Glyceric acid	O <sub>2</sub>	Pt/MCN	3	40	[34]
		O <sub>2</sub>	Pt/SiO <sub>2</sub>	1	100	[33]
		O <sub>2</sub>	AuPdCZ	3	60	[35]
		O <sub>2</sub>	Ag/Al <sub>2</sub> O <sub>3</sub>	5	60	[36]
		O <sub>2</sub>	Au/Al <sub>2</sub> O <sub>3</sub>	5	60	[36]
		O <sub>2</sub>	Pd/Al <sub>2</sub> O <sub>3</sub>	5	60	[36]
		O <sub>2</sub>	Pt/Al <sub>2</sub> O <sub>3</sub>	5	60	[36]
		O <sub>2</sub>	Au/G	5	80	[37]
		O <sub>2</sub>	Au/CNF-R	5	80	[37]
		O <sub>2</sub>	Au/CNS	5	80	[37]
	Glycolic acid	O <sub>2</sub>	Au–Pt	3	60	[38]
		O <sub>2</sub>	AuPdCZ	3	60	[35]
		O <sub>2</sub>	Ag/Al <sub>2</sub> O <sub>3</sub>	5	60	[36]
		O <sub>2</sub>	Au/Al <sub>2</sub> O <sub>3</sub>	5	60	[36]
		O <sub>2</sub>	Pd/Al <sub>2</sub> O <sub>3</sub>	5	60	[36]
		O <sub>2</sub>	Pt/Al <sub>2</sub> O <sub>3</sub>	5	60	[36]
		O <sub>2</sub>	Au/G	5	80	[37]
		O <sub>2</sub>	Au/CNF-R	5	80	[37]
		O <sub>2</sub>	Au/CNS	5	80	[37]
		Hydroxypyruvic acid	O <sub>2</sub>	PtBi/C	–	–
	O <sub>2</sub>		Au/G	5	80	[37]
	O <sub>2</sub>		Au/CNF-R	5	80	[37]
	O <sub>2</sub>		Au/CNS	5	80	[37]
	Mesoxalic acid	O <sub>2</sub>	PtBi/C	–	–	[39]
O <sub>2</sub>		Au/G	5	80	[37]	
O <sub>2</sub>		Au/CNF-R	5	80	[37]	
O <sub>2</sub>		Au/CNS	5	80	[37]	
Oxalic acid	O <sub>2</sub>	AuPdCZ	3	60	[35]	
Tartronic acid	O <sub>2</sub>	Ag/Al <sub>2</sub> O <sub>3</sub>	5	60	[36]	
	O <sub>2</sub>	Au/Al <sub>2</sub> O <sub>3</sub>	5	60	[36]	
	O <sub>2</sub>	Pd/Al <sub>2</sub> O <sub>3</sub>	5	60	[36]	
	O <sub>2</sub>	Pt/Al <sub>2</sub> O <sub>3</sub>	5	60	[36]	
	O <sub>2</sub>	Au/G	5	80	[37]	
	O <sub>2</sub>	Au/CNF-R	5	80	[37]	
	O <sub>2</sub>	Au/CNS	5	80	[37]	
Glycerol reduction	1,2-propanediol	H <sub>2</sub>	Ru/Al <sub>2</sub> O <sub>3</sub>	25	180	[40]
	1,3-propanediol	H <sub>2</sub>	Ru/Al <sub>2</sub> O <sub>3</sub>	80	240	[41]
	Ethylene glycol	H <sub>2</sub>	Ru/Al <sub>2</sub> O <sub>3</sub>	25	200	[42]
		H <sub>2</sub>	Ru/ZrO <sub>2</sub>	80	240	[35]
		H <sub>2</sub>	Ru/ZrO <sub>2</sub>	25	200	[42]
		H <sub>2</sub>	Ru/C	80	130	[43]
		H <sub>2</sub>	3% Ru–0.19% Cu/Al <sub>2</sub> O <sub>3</sub>	100	180	[44]
		H <sub>2</sub>	3% Ru–1% Cu/Al <sub>2</sub> O <sub>3</sub>	80	230	[45]
		H <sub>2</sub>	3% Ru–0.19% Cu/ZrO <sub>2</sub>	100	180	[44]
		H <sub>2</sub>	2.5% Ru–2.5% Cu/Al <sub>2</sub> O <sub>3</sub>	25	200	[42]

Table 3. Cont.

Reaction Type	Product	Reactant	Catalyst	<i>P</i> (bar)	<i>T</i> (°C)	Ref.
Glycerol dehydrogenation	Acrolein	–	AlPO <sub>4</sub> -450	1	190–230	[46]
		–	AlPO <sub>4</sub> -650	1	190–230	[46]
		–	H-ZSM-5(50)	1	170–230	[46]
		–	H-ZSM-5(30)	1	170–230	[46]
		–	HY(5.2)	1	170–230	[46]
		–	12 wt % V <sub>2</sub> O <sub>5</sub> , V/P molar ratio of 0.2	1	325	[47]
Glycerol halogenation	1,3-dichloropropanol	HCl	Aspartic acid	4.5	100	[48]
		HCl	Glutamic acid	4.5	100	[48]
		HCl	Cystein	4.5	100	[48]
		HCl	Glycolic acid	4.5	100	[48]
		HCl	Diglycolic acid	4.5	100	[48]
		HCl	Thioglycolic acid	4.5	100	[48]
Glycerol esterification	Monoglycerides	Acetic acid	Sb <sub>2</sub> O <sub>5</sub>	1	80–120	[49]
		Palmitic acid	ZrSBA-15	1	160–180	[50]
		Acetic acid	Graphene oxide	1	120	[51]
	Diacylglycerol	Acetic acid	ZSM-48	1	120	[51]
		Acetic acid	ZSM-5	1	120	[51]
		Acetic acid	H-mordenite	1	120	[51]
		Acetic acid	WO <sub>3</sub> /ZrO <sub>2</sub>	1	120	[51]
		Acetic acid	MoO <sub>3</sub> /ZrO <sub>2</sub>	1	120	[51]
		Acetic acid	HPW/ZrO <sub>2</sub>	1	120	[51]
		Acetic acid	Cs <sub>2.5</sub> PW	1	120	[51]
		Glycerol carbonate	diethyl carbonate	1-Ethyl-3-methylimidazolium acetate	1	120
diethyl carbonate	1,8-diazabicyclo [5.4.0] undecenc-7-ene (DBU)-methanol		1	100	[53]	
diethyl carbonate	CeO <sub>2</sub>		40	90–190	[54]	
Glycerol pyrolysis	Syngas	–	Bituminous carbon	1	400–900	[55]
		–	Coconut shell	1	400–900	[55]

Therefore, an intensive research work has been addressed in order to investigate the conversion of glycerol to valuable chemicals and Table 3 summarizes some of the most active catalysts for the conversion of glycerol via oxidation, reduction, dehydrogenation, halogenation, esterification and pyrolysis. In detail, the oxidation of glycerol leads to a large number of products such as dihydroxyacetone, glyceric acid, glyceraldehyde, hydroxypyruvic acid, glycolic acid, etc. The control of reaction selectivity represents a key issue to obtain the desired compounds. For example, glyceric acid is an important intermediate for more deeply oxidized products such as tartronic acid and mesoxalic acid [30,34–37]. The catalytic aerobic oxidation of glycerol has been intensively investigated using monometallic or bimetallic catalysts such as Au, Pt, and Pd in a basic medium and some of the most representative catalysts [30–37] used in this field are reported in Table 3.

Another way for obtaining added value products from glycerol is the reduction reaction. Conventionally, this reaction is carried out at medium/high pressures and temperature ranging from 240 to 270 °C over Cu- and Zn-based catalysts promoted by sulfided Ru catalyst [40]. Furthermore, the reduction of glycerol was also studied over catalysts containing Co, Cu, Mn and Mo as well as over homogeneous catalysts containing W and group VIII transition metals. This reaction has been also studied over Cu-Pt and Cu-Ru bimetallic catalysts at mild conditions under reaction pressures of less than 5 MPa and temperatures of less than 200 °C [45]. It was also reported that the glycerol conversion over Cu-based catalysts was lower than Ru-based catalysts. Indeed, the reduction reaction of glycerol over activated carbon or alumina supported Ru catalysts, combined with various solid acid catalysts such as zeolites, sulfated zirconia, rhenium, niobium and an ion exchange resin, have been recently investigated [42], demonstrating that the combination of Ru-based catalysts and solid acid catalysts exhibit high catalytic activity in high pressure over 8 MPa and between 120 °C and around 200 °C (Table 3).



The production of acrolein from glycerol represents an interesting eco-friendly process, which shows some advantages such as a reduction in the oil exploitation and a low impact towards the environment [46]. Generally, the production of acrolein from glycerol is carried out through acid-catalyzed dehydrogenation over synthetic aluminium phosphate ( $\text{AlPO}_4$ ) and zeolites with different channel structures (HY and H-ZSM-5) and  $\text{SiO}_2/\text{Al}_2\text{O}_3$  ratio [45,46].

In recent years, a new synthetic route for the preparation of chlorohydrins, by reacting a polyhydroxy aliphatic hydrocarbon with a chlorination agent has been proposed. In particular, Tesser et al. [48] studied homologous chlorinated series of catalysts for glycerol halogenation, such as acetic acid, monochloroacetic, dichloroacetic, trichloroacetic acid, etc. focusing on both activity and selectivity shown by each catalyst.

Table 3 also contains information about one of the most important processes to convert glycerol such as the esterification with acetic acid to produce monoacylglycerol, diacylglycerol and glycerol carbonate. These products are widely utilized in cryogenics, biodegradable polyester and cosmetics [50,51]. Significant acid catalysts can be used for glycerol esterification, including sulfated based superacids, heteropolyacid-based catalysts, tin chloride, zeolite,  $\text{ZrO}_2$  based solid acids, etc. [50–55]. Unfortunately, most of them show as main drawbacks the rapid deactivation, complex preparation procedures, low reactivity and expensive costs. As a solution to contrast these disadvantages, graphene and graphene oxide have received great attention because highly active, inexpensive, robust and sustainable solid acid catalyst for glycerol esterification [51].

Last but not least, the pyrolysis of glycerol to produce syngas represents another way to convert the glycerol. In the specialized literature, the pyrolysis of biomass has been widely investigated, but in most of cases only metal-based catalysts have been used. A novel method for syngas production is represented by the microwave-assisted pyrolysis of glycerol over a carbonaceous catalyst, in which the heating method and the operating temperature (between 400 and 900 °C) can influence the catalytic effect of the activated carbons in order to maximize syngas production [55].

Regarding the contents of Table 4, in recent years, the need of developing new and alternative polyol production methods has become of great industrial interest and much attention has been paid to biochemical processes. In particular, Table 4 shows a small overview about the most representative products coming from glycerol conversion by fermentation process.

**Table 4.** Products coming from glycerol conversion by fermentation process with related operating conditions (Adapted from [29]).

Product	Utilization	Organism	Fermentation Mode	Oxygen Availability	Yield (Product/Glycerol)	Productivity	Product Concentration	Ref.
<b>1,3-Propanediol</b>	Polytrimethylene terephthalate (PTT), carpets, special textile fibers, monofilaments, films, non-woven fabrics, polybutylene terephthalate (PBT) [56]	<i>C. pasteurianum</i>	Batch	Anaerobic	0.14 g/g	–	4.63 g/L	[57]
		<i>K. pneumoniae</i> DSM 2026	Fed-batch	Microaerobic	0.52 mol/mol	1.57 g/L/h	59.50 g/L	[58]
		<i>K. pneumoniae</i> LDH 526	Fed-batch	Aerobic	0.52 mol/mol	2.13 g/L/h	102.1 g/L	[59]
		<i>C. butyricum</i> F2	Batch	Anaerobic	0.53 g/g	1.05 g/L/h	47.1 g/L	[60]
		<i>E. coli</i> K12	Fed-batch	Anaerobic	90.2%	2.61 g/L/h	104.4 g/L	[61]
		<i>K. pneumoniae</i>	Fed-batch	Anaerobic	61 mol/mol	2.2 g/L/h	75 g/L	[62]
		<i>K. pneumoniae</i> G31	Fed-batch	Microaerobic	0.36 mol/mol	0.18 g/L/h	49.2 g/L	[63]
<b>2,3-Butanediol</b>	Plastics, anti-freeze solutions, methyl ethyl ketone production, 1,3-butadiene (used to produce synthetic rubber), diacetyl and to precursors of polyurethane (used in the pharmaceutical and cosmetics industries) [64]	<i>K. pneumoniae</i> G31	Fed-batch	Aerobic	0.39 g/g	0.47 g/L/h	70.0 g/L	[65]
<b>Ethanol</b>	Food and chemical industries [66]	<i>C. pasteurianum</i>	Batch	Anaerobic	0.06 g/g	–	1.87 g/L	[57]
		<i>E. coli</i> SY 4	Batch	Microaerobic	85%	0.15 g/L/h	7.8 g/L	[67]
		<i>C. pasteurianum</i>	Batch	Anaerobic	0.29 g/g	–	7.85 g/L	[57]
<b>Butanol</b>	Paints, lacquers, and resin formulations [68]	<i>C. pasteurianum</i>	Batch	Anaerobic	0.36 g/g	–	1.8 g/L	[69]
		<i>C. pasteurianum</i> DSM 525	Batch	Anaerobic	0.34 mol/mol	–	7 g/L	[70]
<b>Dihydroxyacetone</b>	Skin care products [71]	<i>G. oxydans</i> ZJB09112	Fed-batch	Aerobic	88.7%	–	161.9 g/L	[72]
<b>Glyceric acid</b>	Chemical and pharmaceutical industries and for the production of polymers [73]	<i>G. frateurii</i> NBRC103465	Fed-batch	Aerobic	0.76 g/g	0.81 g/L/h	136.5 g/L	[74]
		<i>A. tropicalis</i> NBRC16470	Fed-batch	Aerobic	0.46 g/g	0.71 g/L/h	101.8 g/L	[74]
<b>Lactic acid</b>	Food industry, acrylic acid and 1,2 propanediol used in polyester resins and polyurethane [75]	<i>E. coli</i> AC-521	Fed-batch	Aerobic	0.9 mol/mol	0.49 g/g/h	85.8 g/L	[76]
		<i>E. coli</i> LA02Δdld	Batch	Microaerobic	0.83 g/g	1.25 g/g/h	32 g/L	[77]
<b>Succinic acid</b>	Pharmaceuticals, antibiotics, amino acids, vitamins, green solvents, and biodegradable plastics [78]	engineered <i>E. coli</i>	Batch	Microaerobic	0.69 g/g	~4 g/g/h	14 g/L	[79]
		<i>Y. lipolytica</i> Y-3314	Batch	Oxygen limited	0.45 g/g	–	45 g/L	[80]
<b>Citric acid</b>	agro-industrial products [81]	<i>Y. lipolytica</i>	Repeated batch	Aerobic	0.77 g/g	0.85 g/L/h	124.2 g/L	[82]
<b>Oxalic acid</b>	Manufacture industries, paper and detergents industries [83]	<i>A. niger</i>	Batch	Aerobic	0.62 g/g	–	21 g/L	[84]
<b>Mannitol</b>	Food and pharmaceutical industries [85]	<i>C. magnoliae</i>	Batch	Aerobic	0.51 g/g	0.53 g/L/h	51 g/L	[86]
<b>Erythritol</b>	Food industries [87]	<i>Y. lipolytica</i> Wratislavia K1	Fed-batch	Aerobic	0.56 g/g	1.0 g/L/h	170 g/L	[88]
<b>Arabitol</b>	Food industries [89]	<i>D. hansenii</i> SBP1	Batch	Aerobic	0.50 g/g	0.12 g/L/h	14 g/L	[89]
<b>PHB</b>	Production of polymers [90]	<i>E. coli</i> Arc2	Fed-batch	Microaerobic	–	0.18 g/L/h	10.81 g/L	[91]
		<i>Z. denitrificans</i> MW1	Fed-batch	Aerobic	0.25 g/g	1.09 g/L/h	54.3 g/L	[92]

Among the engineered strains, 1,3-propanediol production from glycerol using *K. pneumoniae* and *E. coli* strains is considered one of the most promising methods [29]. It is influenced by the purity and concentration of the glycerol as well as by fermentation conditions. Furthermore, as reported in Table 4, also 2,3-butanediol can be obtained as a major product of glycerol fermentation by *K. pneumoniae* [65]. Bacteria of the *Enterobacteriaceae* family and the *Clostridium* genus are useful to convert glycerol to ethanol, even though their yields are relatively low since ethanol represents only a secondary product of the fermentation, while the main products are 1,3-propanediol and 2,3-butanediol. Nevertheless, *E. coli* can transform glycerol to ethanol anaerobically as well as aerobically. Glycerol conversion of about 85% to ethanol (i.e., yield, Table 4) is then possible, demonstrating the potentiality of using *E. coli* as a host for the production of ethanol from glycerol. Butanol represents a key chemical platform, because industrially convertible to acrylates, ethers, and butyl acetate, etc. *C. pasteurianum* can be considered for producing butanol when grown in crude glycerol, although butanol yields and productivity on this substrate is considerably lower than on glycerol. However, another important chemical produced from glycerol fermentation is the dihydroxyacetone, which represents the main active ingredient in all sunless tanning skincare products. As the dihydroxyacetone, glyceric acid is biotechnologically produced mainly by the family of acetic acid bacteria, while recently *E. coli* has been engineered for homofermentative production of lactic acid from glycerol. Succinic acid is widely used for manufacturing health-related products, including pharmaceuticals, antibiotics, amino acids, and vitamins [80]. A recent approach in the production of succinic acid is related to the exploitation of yeast in an aerobic recombinant strain via *Yarrowia lipolytica*, able to produce succinic acid when cultivated on glycerol at low pH. As for the succinic acid, the yeast *Yarrowia lipolytica* has gained much attention in recent years because it is able to metabolize several important industrial and agro-industrial byproducts to produce organic acids such as citric acid, which is considered a weak organic acid, commercially produced by fermentation of molasses.

Oxalic acid is an organic acid useful in industry for the manufacture of paper and detergents [84]. Its production can take place by *Aspergillus niger* growing in crude glycerol waste from biodiesel production plants. *Candida magnoliae* is an excellent mannitol producer using glucose and fructose mixtures as carbon sources. Furthermore, mannitol production from glycerol using *C. magnoliae* can show a consume of 100 g/L of glycerol in 96 h, resulting in 51 g/L of mannitol, corresponding to a yield of 0.51 g/g. Commercial erythritol is produced exclusively via fermentation in substrates containing sugars, such as glucose and fructose, from the hydrolysis of biomass. In case of using residual crude glycerol, an acetate-negative mutant of *Y. lipolytica* (Wratislavia K1) is able to simultaneously produce significant quantities of erythritol and citric acid, while the arabitol production by *D. hansenii* SBP-1 can achieve a yield of 0.5 g/g.

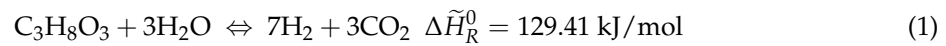
The last part of Table 4 contains indications about the polyhydroxyalkanoates, which have received great attention due to their potential application as renewable, biodegradable, and biocompatible thermoplastics. Poly-3-hydroxybutyrate (PHB) belongs to the group of polyhydroxyalkanoates and represents the most significative example of biodegradable polyesters [92]. Conversion of glycerol to PHBs has reached high production levels due to optimization of strains and fermentations conditions. In particular, fed-batch cultivation improves PHB production by using the *Zobellella denitrificans* MW1, which is characterized by a large amount of PHB from glycerol in presence of NaCl.

However, glycerol can be further used for producing H<sub>2</sub> via steam reforming, partial oxidation and pyrolysis reactions [93–161]. In the next part of the review, particular attention is devoted to this task, with particular emphasis on steam reforming reactions.

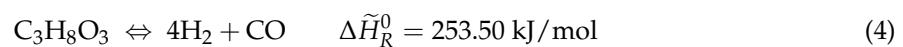
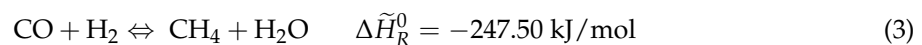
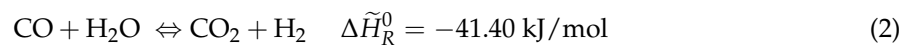
## 2. Steam Reforming of Glycerol for Hydrogen Production

### 2.1. Thermodynamic

As also indicated in previous thermodynamic analyses [143,146,161], glycerol steam reforming (GSR) reaction takes place within glycerol and steam to produce hydrogen and carbon dioxide (1):



Alongside, secondary reactions such as Water Gas Shift (WGS) (2), methanation (3) and glycerol pyrolysis (4) can occur:



The GSR reaction (1) evolves towards the products with an increment of moles number and, hence, it is favoured at low pressure and, due to its endothermic nature, it is promoted at higher temperature.

All the aforementioned four reactions are limited by the thermodynamic equilibrium; therefore, the differential equation to the Gibbs free energy for single phase applies:

$$d(nG) = (nV)dP - (nS)dT + \sum_i \mu_i dn_i \quad (5)$$

In equilibrium closed system, at constant temperature and pressure, Equation (5) can be reduced to (6):

$$\sum_i \mu_i dn_i = 0 \quad (6)$$

and if manipulated, it becomes:

$$\ln \prod_{i=1} \left( \frac{\hat{f}_i}{f_i^o} \right)^{\nu_i} = \frac{-\sum_i \nu_i G_i^o}{RT} = \ln(K) \quad (7)$$

Equations (6) and (7) can be written for each one of the aforementioned reaction. As a consequence, the thermodynamic data, can be used to show the influence of temperature and pressure on the reaction performance in terms of H<sub>2</sub> yield and selectivity for *i*-compound, as shown in Figure 10, where H<sub>2</sub> yield and selectivity are defined as follows:

$$\text{H}_2\text{yield} = \frac{\text{H}_2\text{moles produced}}{7 \text{ moles glycerol in feed}} \times 100 = [\%] \quad (8)$$

$$S_i = \frac{\text{moles of } i\text{-compound}}{\text{CH}_4 + \text{CO} + \text{CO}_2} = [-] \quad (9)$$

The process endothermicity is clearly depicted in Figure 10a,b, since the best yields were obtained at high temperature. Figure 10b shows that, when the pressure increases the methane production improves (undesired reaction (3)). Furthermore, focusing on carbon dioxide yield at 5 bar, it can be seen that the maximum yield is obtained between 550 and 700 °C, indicating that Equation (2) is favoured among the other reactions. Varying the water/glycerol molar ratio (WGMR) between 3 and 9, the higher the WGMR the higher the hydrogen yield (Figure 10c).

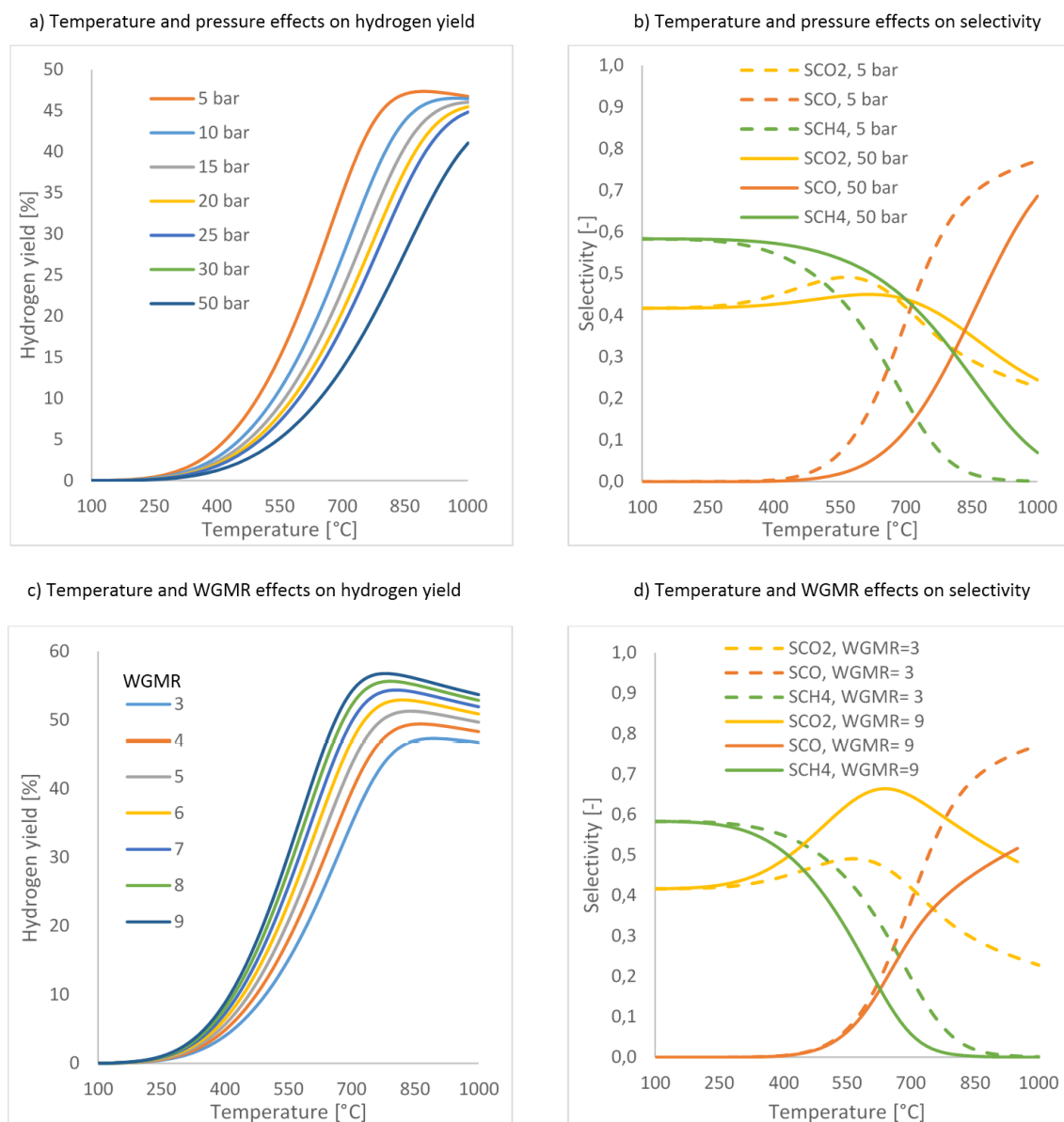


**Figure 10.** Thermodynamic analysis about GSR reaction performance in terms of hydrogen yield and selectivity: effect of pressure, temperature and water/glycerol molar ratio (WGMR). (a) temperature and pressure effects on hydrogen yield; (b) temperature and pressure effects on hydrogen selectivity; (c) temperature and WGSMR effects on hydrogen yield; (d) temperature and WGSMR effects on selectivity.

## 2.2. Kinetics and Catalysts Used to Perform GSR Reaction

In the specialized literature about GSR reaction, the heterogeneous catalysts used to perform this process are similar to those used in steam reforming of methane (SRM), such as Ni, Ru, Co, etc. It is worth noting that interesting critical reviews in this field have been already published, highlighting most of the mono and bimetallic catalysts useful for GSR reaction [155–158].

Table 5 details a brief overview of GSR reaction catalysts, pointing out the values of activation energy, reaction rate and the reaction order for glycerol and water.

Table 5. Typical catalysts for GSR reaction.

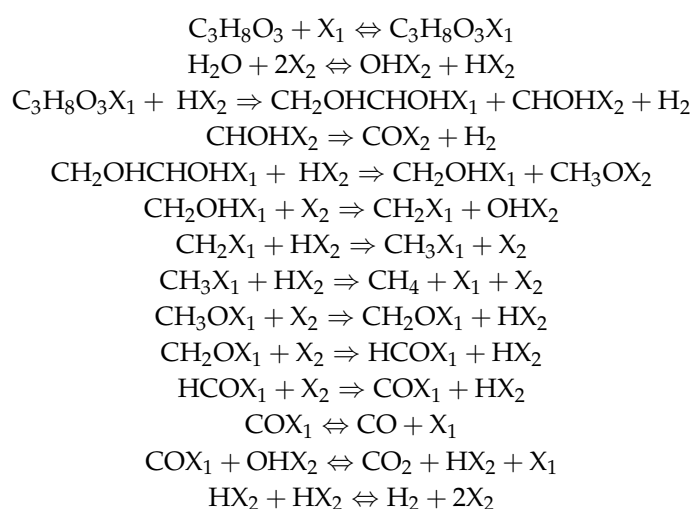
Catalyst Type	$\alpha$ *	$\beta$ **	$E_a$ (kJ/mol)	Ref.
Pt/C	1	–	–	[93]
Co/Al <sub>2</sub> O <sub>3</sub>	0.10	0.4	67.2	[94]
Ni/Al <sub>2</sub> O <sub>3</sub>	0.48	0.34	60.0	[95]
Co-Ni/Al <sub>2</sub> O <sub>3</sub>	0.25	0.36	63.3	[96]
Ni/CeO <sub>2</sub>	0.233	–	103.4	[97]
Ni-ZrO <sub>2</sub> /CeO <sub>2</sub>	0.3	–	43.4	[98]
NiO-MgO/Al <sub>2</sub> O <sub>3</sub> 45.1-24.1/30.8	0.895	–	131.6	[99]
NiO-MgO/Al <sub>2</sub> O <sub>3</sub> 34.4-18.5/47.1	0.936	–	74.6	[100]
NiO-MgO/Al <sub>2</sub> O <sub>3</sub> 24.1-26.1/49.8	0.977	–	37.8	[100]

\* reaction order for glycerol, \*\* reaction order for water.

A critical issue about GSR reaction is represented by coke deposition and subsequent catalysts deactivation. In the following subparagraph, this task is discussed in brief, but deeper information can be found in Gallo et al. [159], who proposed some catalyst modifications able to reduce catalysts coking, or in Bossola et al. [160], who pointed out a different approach involving a pyrolytic pretreatment step before reformers.

### 2.2.1. Nickel catalyst in GSR reaction

Ni-based catalysts are studied widely for several reaction processes. Specifically, Cheng et al. [95] proposed a reaction mechanism for the GSR reaction in the presence of Ni on alumina catalyst using kinetics expression of Langmuir-Hinshelwood. The mechanism is described as follows:



Glycerol is absorbed on a catalytic site and it is dissociated into hydrogen and hydroxyl. After that, the absorbed glycerol reacts with the hydrogen absorbed to dissociate into simpler molecules to produce hydrogen and carbon dioxide, which is desorbed at the end of the process. Furthermore, they proposed two kinetic equation models, of which, one of them is based on the reaction mechanism previously illustrated:

$$r = \frac{k_{rxn} P_G \sqrt{P_W}}{(1 + K_G P_G)(1 + \sqrt{K_W P_W})} \quad (10)$$

where  $k_{rxn}$ ,  $K_G$  and  $K_W$  are equal to  $1.33 \times 10^{-7} \text{ mol} \cdot \text{m}^{-2} \cdot \text{s}^{-1} \cdot \text{kPa}^{-1}$ ,  $5.60 \times 10^{-4} \text{ kPa}^{-1}$  and  $0.043 \text{ kPa}^{-1}$ , respectively.

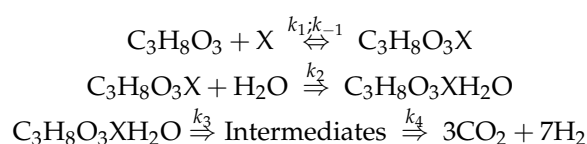
Wang et al. [14] studied a GSR catalyst based on NiO 24.1 wt %, MgO 26.1 wt % and Al<sub>2</sub>O<sub>3</sub> 49.8 wt %. At 650 °C, the catalyst exhibits a H<sub>2</sub> selectivity of 78.5% and glycerol conversion of 88.0%. Dieuzeide et al. [101,102] investigated the influence of Mg presence in Ni-Mg/Al<sub>2</sub>O<sub>3</sub> catalyst, varying

its weight percentage in the range 0%–10%. At 500 °C and WGMR = 3.5/1, they observed the best result in terms of low carbon formation by using the catalyst loaded with 3 wt % of Mg, probably because it favours a better Ni dispersion. Seung-hoon et al. [103] added alkaline metals (K, Ca, Sr) as promoters in Ni/Al<sub>2</sub>O<sub>3</sub> catalyst. A very low carbon coke formation was obtained by using Sr-Ni/Al<sub>2</sub>O<sub>3</sub>, probably as a consequence of a basicity increment of the whole catalyst. Huang et al. [104] prepared a Ni-based catalysts using commercial Ca-containing Linde-type 5A zeolite (LTA) as support, in presence of Mo–La oxides and CaO to demonstrate that an increase on basic property of Ni/LTA catalysts helps to improving glycerol conversion to syngas and inhibits water–gas shift reaction and methanation during GSR. Gallegos-Suárez et al. [105] tested a NiO (between 5 and 30 wt %) catalysts supported on MgO and CeO<sub>2</sub> for GSR reaction at different temperature from 250 to 550 °C, weight hourly space velocity (WHSV) = 5.3 h<sup>-1</sup>, WGMR = 16/1, in a fixed-bed reactor. They reached 80% as a maximum glycerol conversion at 550 °C using a 15% NiO catalyst, while glycerol conversion (~15%) decreased due to an increment of carbon coke formation. Shao et al. [106] tested a Ni/CeZr catalyst with different weight percentage of supports to improve the catalytic stability and minimize the carbon coke formation. Kousi et al. [107] investigated the effects of B<sub>2</sub>O<sub>3</sub> and La<sub>2</sub>O<sub>3</sub> on Ni/Al<sub>2</sub>O<sub>3</sub> catalyst during GSR reaction, observing an increment of the hydrogen yield in presence of La<sub>2</sub>O<sub>3</sub>, while by adding B<sub>2</sub>O<sub>3</sub> the authors noted an inverse result, more pronounced at lower temperatures (~400 °C). Bobadilla et al. [108] studied a Ni-Sn bimetallic catalyst supported over Al<sub>2</sub>O<sub>3</sub> modified with different promoter (Mg and/or Ce). GSR reaction was then performed at 650 °C, 1 bar and WGMR = 12, observing that the addition of MgO and CeO<sub>2</sub> made a synergetic effect possible, able to decrease the coke formation by suppression of Lewis acids centres and favouring the WGS reaction. Go et al. [109] studied three different Ni-based catalysts: Ni-Fe-Ce/Al<sub>2</sub>O<sub>3</sub>, Ni-Fe-La/Al<sub>2</sub>O<sub>3</sub> and Ni-Fe-Cr/Al<sub>2</sub>O<sub>3</sub>. During GSR reaction, Ni-Fe-Ce/Al<sub>2</sub>O<sub>3</sub> shows low carbon coke formation at high temperature.

Ni and Ni-Pd catalysts supported on Al<sub>2</sub>O<sub>3</sub>-ZrO<sub>2</sub>, Al<sub>2</sub>O<sub>3</sub>-ZrO<sub>2</sub>-La<sub>2</sub>O<sub>3</sub> and on Olivine have been compared by Yurdakul et al. [110] studying the influence of the support with the temperature. In the temperature range between 600 and 800 °C and at WGMR = 5/1 they reached the maximum H<sub>2</sub> yield, about 74%, using the Ni-Pd/Al<sub>2</sub>O<sub>3</sub>-ZrO<sub>2</sub> catalyst. Meanwhile, the presence of La<sub>2</sub>O<sub>3</sub> decreased the CO<sub>2</sub> selectivity, resulting unfavourable for the GSR reaction.

### 2.2.2. Ruthenium Catalyst in GSR Reaction

The reaction mechanism of the GSR reaction in presence of Ru-based catalyst has been proposed by Sundari et al. [111] as follows:



The glycerol (A) is absorbed on the catalyst surface with water (B) creating a complex that, successively, reacts to form CO<sub>2</sub> and H<sub>2</sub>. In this case, the reaction rate is:

$$r = \frac{k_1 k_2 p_A p_B}{k_{-1} + k_1 p_A + k_2 p_B + k_1 k_2 p_A p_B / k_3} \quad (11)$$

At high WGMR, the water partial pressure can be assumed constant ( $p_B = p_{B0}$ ), so the reaction rate can be rewritten as:

$$r = \frac{k_R p_A}{1 + b p_A} \quad (12)$$

where  $k_R$  and  $b$  coefficient can be defined as:

$$k_R = \frac{k_1 k_2 p_{B0}}{k_{-1} + k_2 p_{B0}}; b = \frac{k_1 + (k_1 k_2 p_{B0} / k_3)}{k_{-1} + k_2 p_{B0}} \quad (13)$$



As a consequence, for low glycerol partial pressure  $bp_A \ll 1$ , the kinetic rate results to be of the first order (see Equation [13]).

Hirai et al. [112] studied GSR reaction by using Ru catalyst and analysing the effect of different kind of supports ( $Y_2O_3$ ,  $ZrO_2$ ,  $CeO_2$ ,  $SiO_2$ ,  $MgO$  and  $Al_2O_3$ ), pointing out that Ru/ $Y_2O_3$  made the best performance possible with  $H_2$  yield about 90% at 600 °C.

### 2.2.3. Cobalt Catalyst in GSR Reaction

Even though cobalt catalysts do not represent the best solution to carry out GSR reaction, Sanchez et al. [113] studied a bimetallic catalyst, Ni(4 wt %)-Co(4, and 12 wt %), supported on  $\gamma-Al_2O_3$ . However, in this study, the authors evidenced that cobalt acts as a precursor, while the catalytic activity is mainly given by Ni. These catalysts favoured the production of  $H_2$  as the main product, with  $CO_2$ ,  $CO$  and  $CH_4$  found in smaller concentrations. In particular, the presence of Co promoted  $H_2$  production and reduced  $CO_2$  formation by decreasing the reaction temperature with a depletion of  $CH_4$  formation. The low Co loading produced the largest  $H_2$  and  $CO_2$  amounts at relatively low temperature, with low  $CO$  and  $CH_4$ . In contrast, high Co loading maximised the  $H_2$  production, depleting  $CO_2$  formation, at relatively low temperature.

Also, Araque et al. [114] used a bimetallic Co-based catalyst (Co-Rh) for the production of hydrogen from GSR reaction. In this case, the cobalt catalyst allowed the selective production of  $H_2$ , where the presence of Rh favoured the stability of the catalyst.

### 2.2.4. Platinum Catalyst in GSR Reaction

Regarding the utilization of Pt-based catalyst in GSR reaction, Pompeo et al. [115] described an interesting mechanism, represented schematically in Figure 11. The mechanism involves two paths: the first pathway (I) consists of a dehydrogenation of glycerol with subsequent dehydration to form acetol; a second dehydrogenation, with a first breaking of C–C bond and subsequent formation of acetic acid (caused by a dehydrogenation and cleavage of the C–C bond). Then, the acetic acid decomposes into  $CO_2$  and  $H_2$ . The second pathway [II] does not involve dehydration reactions, but mainly cleavage of C–C bonds and dehydrogenations, producing  $H_2$  and  $CO$ . The same mechanism has been proposed for Ni-based catalyst [116].

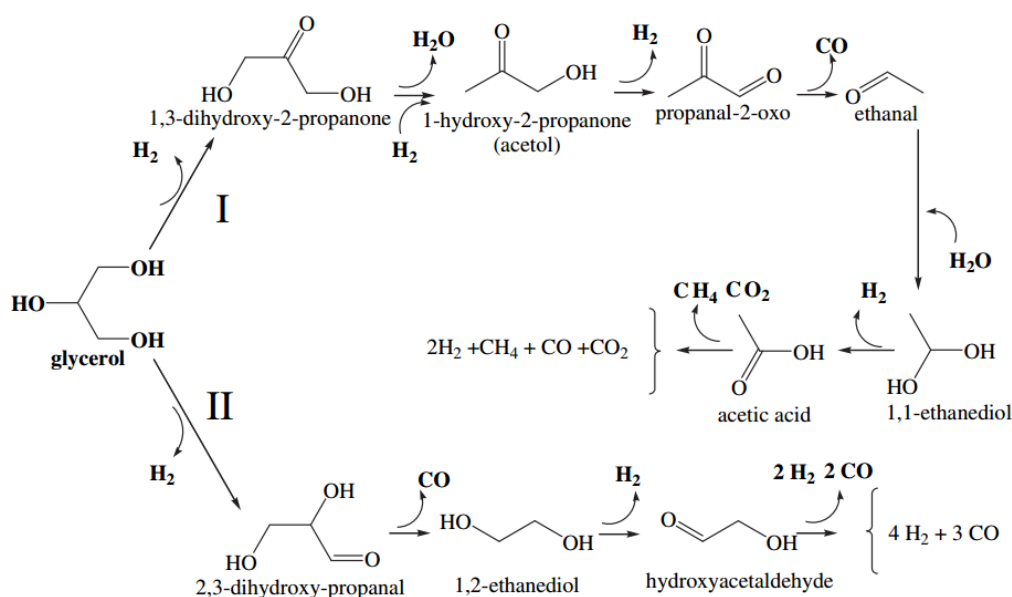


**Figure 11.** Reaction mechanism during GSR reaction using Pt-based catalysts. With permission of reprint by Elsevier from [115].



Pastor-Pérez et al. [117] prepared some bimetallic PtSn/C catalysts with different Sn/Pt atomic ratios (0.2, 0.3, 0.5, and 0.7) for improving the catalytic activity, selectivity and/or stability. They reached the maximum H<sub>2</sub> yield (about 36%) for GSR at 1 bar, 350 °C and WGMR = 9/1 and 0.2 as Sn/Pt atomic ratio.

Sad et al. [118] optimized the Pt-based catalyst used for GSR reaction, changing different type of supports such as SiO<sub>2</sub>, MgO, Al<sub>2</sub>O<sub>3</sub> and TiO<sub>2</sub> between 300 and 350 °C. The most important result is the total glycerol conversion, with higher H<sub>2</sub> yield in case of Pt/SiO<sub>2</sub> utilization.

### 2.2.5. Perovskites in GSR Reaction

Surendar et al. [119] doped cobalt based perovskites (LaCo<sub>0.99</sub>X<sub>0.01</sub>O<sub>3</sub>) with X = Au, Ag, Cu and Pt to study GSR reaction between 400 and 700 °C, achieving the best performance in terms of hydrogen yield (~78%) and glycerol conversion (~96%). Furthermore, they demonstrated that the carbon coke formation varies depending on the type of metal dopant as in the following scale: LaCoO<sub>3</sub> > Au > Ag > Cu ~ Pt.

Ramesh et al. [120] used perovskite catalysts for this reaction at low temperature, specifically LaNi<sub>X</sub>Cu<sub>Y</sub>O<sub>3</sub> (X between 0.5 and 1 and Y between 0 and 0.5). The goal of the authors was given by the utilization of Ni as reformer catalyst, LaO<sub>3</sub> to decrease the reaction temperature and Cu to improve the stability of the catalyst and favour a low carbon coke formation. They achieved interesting performance utilizing LaNi<sub>0.9</sub>Cu<sub>0.1</sub>O<sub>3</sub> at 650 °C in terms of glycerol conversion and H<sub>2</sub> selectivity (73.0% and 67.3%, respectively).

Mitran et al. [121] used molybdena-alumina based catalysts at 400–500 °C with WGMR between 9:1 and 20:1 and feed flow rate 0.04–0.08 mL/min. They obtained the best results at maximum percentage of molybdena, WGMR, temperature and lowest feed flow rate, with CH<sub>4</sub> selectivity less than 5%.

## 3. Innovative Technologies for Producing H<sub>2</sub> from Steam Reforming of Glycerol

### 3.1. Membranes and Membrane Reactors

Among the various alternative technologies to the conventional systems for producing hydrogen by a green process, membrane reactor (MR) technology plays an important role in terms of Process Intensification Strategy because it involves a unique operation unit to perform both the chemical reaction and the hydrogen separation/purification process [122,123]. Thus, using MRs the plants are more compact with lower investment costs and cost-effective process [124]. The presence of the membrane, in an equilibrium restricted reaction, makes possible to overcome the thermodynamic equilibrium conversion of the equivalent conventional reactor: This is due to the selective removal of a product from the reaction system, acting a shift effect on the reaction itself, which proceeds with a higher products formation (with consequent conversion improvement).

Another functionality of the MRs is represented by the control of reactants addition for permeation through the membrane, avoiding the disadvantage of secondary reactions and increasing the overall reaction.

The membrane can be classified according to its nature, geometry and the type of transport mechanism [125] as follows:

- macroporous membranes, with a pore size greater than 50 nm;
- mesoporous membranes, with a pore size between 2 and 50 nm;
- microporous membranes, with smaller pore size of 2 nm;
- dense membranes, with pore size <0.5 nm.

For dense membranes, the transport mechanism is represented by solution-diffusion, while in porous membranes different types of transport mechanisms often compete with each other to control

the process [126,127]. In the following section, we report some of the most common mechanism used for describing a gas permeation process through porous membranes:

- Poiseuille mechanism. It takes place when the average pore diameter is much larger than the mean free path of the molecules; therefore, the collisions within the various molecules are more frequent than those within molecules and porous walls:

$$J_i = -\frac{\varepsilon \times d_{pore}^2}{32 \times R \times T \times \eta \times \tau} p \nabla p \quad (14)$$

where  $\varepsilon$  = membrane void fraction,  $d_{pore}^2$  = pore diameter,  $R$  = universal constant,  $T$  = temperature,  $p$  = pressure,  $\tau$  = tortuosity,  $\nabla p$  = pressure gradient and  $\eta$  = viscosity.

- Knudsen diffusion mechanism. When the pores diameters are comparable or less than the mean free path, the quantum momentum is transferred by the collisions between the molecules and the wall of the pores. Applying the kinetic theory of gases to a single straight and cylindrical pore, the Knudsen diffusion coefficient can be defined as:

$$D_{i,K} = \frac{\varepsilon \times d_{pore}}{3 \times \tau} \sqrt{\frac{8 \times R \times T}{\pi \times MW_i}} \quad (15)$$

where  $\varepsilon$  = membrane void fraction,  $d_{pore}$  = pore diameter,  $R$  = universal constant,  $\tau$  = tortuosity,  $\eta$  = viscosity and  $MW$  = molecular weight.

As a special field of interest, metallic membranes are particularly involved in hydrogen separation/purification field due to the characteristics of hydrogen perm-selectivity of dense metallic layers [128]. As useful material for membrane fabrication, Pd and its alloys have been extensively studied [129]. However, as high the hydrogen perm-selectivity over all of the other gases as low the permeability (and vice versa), while the cost of the membranes strictly depends on the thickness of membrane material (Pd, Pd-alloy). In the last two decades, composite Pd-based membranes consisting of thin metal films coated over porous supports have been particularly studied because exhibiting high hydrogen permeability and selectivity values depending on the Pd-alloy layer covering the porous support [130,131].

MR technology has been and is particularly used in hydrogen production from the reforming of hydrocarbons and/or alcohols. As a consequence, the utilisation of self-supported and composite Pd-based membranes showing full hydrogen perm-selectivity and high permeability allows for both high-grade hydrogen stream and hydrogen recovery as well.

#### Pd-Based Membrane Reactors for H<sub>2</sub> Production

In the last 50 years, several companies as Johnson Matthey moved from the commercialization of unsupported dense Pd-based membranes to composite thin Pd-layer supported on porous substrates, matching the objective of producing more mechanical resistant and cost effective Pd-membranes for potential industrial applications [132]. The transport mechanism of the hydrogen permeation through a dense layer of palladium or its alloy (Figure 12) is represented by the solution-diffusion, which takes place specifically in six steps as resumed below:

1. H<sub>2</sub> molecules adsorption from the membrane side at higher H<sub>2</sub> partial pressure;
2. Dissociation of H<sub>2</sub> molecules on the surface;
3. Reversible dissociative chemisorption of atomic H<sub>2</sub>;
4. Reversible dissolution of atomic H<sub>2</sub> in the metal lattice of the membrane;
5. Diffusion into the metal of atomic H<sub>2</sub> proceeds from the side of the membrane at a higher H<sub>2</sub> pressure to the side at lower pressure;
6. Desorption of re-combined atomic H<sub>2</sub> into molecular form.

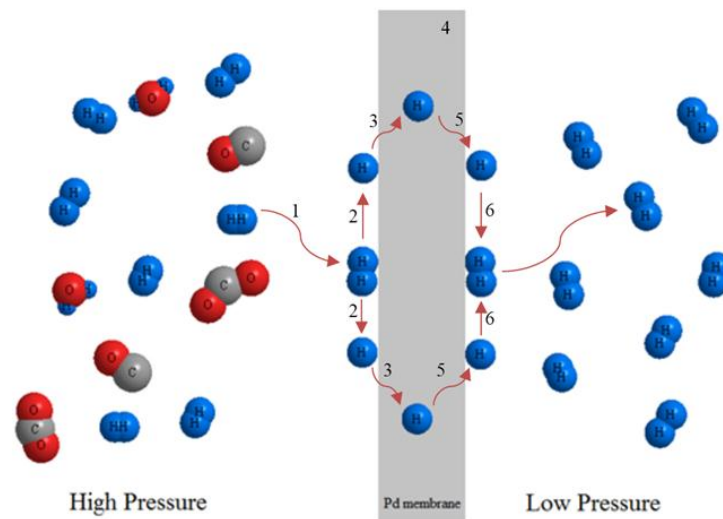


**Figure 12.** Schematic representation of hydrogen permeation through a dense layer of palladium.

From a theoretical point of view, the solution-diffusion mechanism evolves in three main types of fluxes:

$$J_1 = k_1 p_{H_2,1} - k_2 \bar{p}_{H_2,1}^2 \tag{16}$$

$$J_2 = k_2 \bar{p}_{H_2,2} - k_1 p_{H_2,2} \tag{17}$$

$$J_3 = D(C_2 - C_1) \tag{18}$$

Equation (16) represents H<sub>2</sub> adsorption on the membrane side at higher partial pressure; Equation (17) denotes the dissociation into atomic H<sub>2</sub>, reversible dissociative chemisorption of atomic H<sub>2</sub> and Equation (18) is the final desorption of recombined H<sub>2</sub> molecules.

At steady state conditions, the aforementioned fluxes are equal ( $J_{H_2} = J_1 = J_2 = J_3$ ) and, by adding  $J_1$  and  $J_2$ :

$$2J_{H_2} = k_1 (p_{H_2,1} - p_{H_2,2}) - k_2 (\bar{p}_{H_2,1}^2 - \bar{p}_{H_2,2}^2) \tag{19}$$

By taking also into account the average dissolved H<sub>2</sub> concentration, the H<sub>2</sub> flux can be expressed as:

$$J_{H_2} = \frac{1}{\alpha_{diff} - \frac{2}{k_1}} (p_{H_2,1} - p_{H_2,2}) \tag{20}$$

where  $\alpha_{diff}$  is a diffusion coefficient describing the relationship between the resistance of H<sub>2</sub> transport on the membrane surface and the H<sub>2</sub> dissociation into the metal lattice,

$$\alpha_{diff} = \frac{Dr^2(k_1/k_2)}{2\delta C_{Av}} \tag{21}$$

Consequently, the H<sub>2</sub> permeating flux can be expressed by the following general equation:

$$J_{H_2} = Pe_{H_2} \frac{(p_{H_2,ret}^n - p_{H_2,perm}^n)}{\delta} \tag{22}$$

where  $Pe_{H_2}$  is the H<sub>2</sub> permeability through the membrane,  $p_{H_2,ret}$  and  $p_{H_2,perm}$  the hydrogen partial pressure in the retentate and permeate sides, respectively, and  $n$  the exponent expressing the dependence of H<sub>2</sub> flux to the H<sub>2</sub> partial pressure (variable between 0.5 and 1) and  $\delta$  the thickness of the palladium layer.

When  $n = 0.5$ , the transport resistance is represented by the  $H_2$  dissociation into the Pd-layer, then Equation (22) becomes the Sieverts-Fick law (see Equation (23)):

$$J_{H_2} = Pe_{H_2} \frac{(p_{H_2,ret}^{0.5} - p_{H_2,perm}^{0.5})}{\delta} \tag{23}$$

Concerning the temperature influence on the  $H_2$  permeability, the relationship between the hydrogen permeation rate and the temperature can be described by the Arrhenius law:

$$Pe_{H_2} = Pe_{H_2}^0 \exp\left(-\frac{E_a}{RT}\right) \tag{24}$$

where  $Pe_{H_2}^0$  and  $E_a$ , are the pre-exponential factor, and the apparent activation energy, respectively.

Steward et al. [133] demonstrated that, when the metals have a body centered cubic (BCC) as a crystal structure (i.e., V, Nb and Ta), they show higher  $H_2$  permeability than the face centered cubic (FCC) metals such as Pd and Ni. Figure 13 reports the  $H_2$  permeability through different dense metals versus temperature. As shown in the graph, the  $H_2$  permeability is inversely proportional to the temperature for V, Nb and Ta, whereas it is directly proportional to the temperature in Pd and Ni.

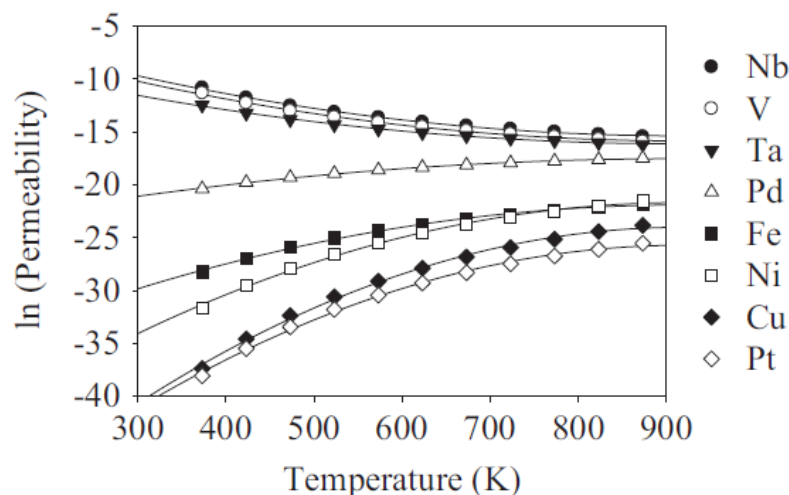


**Figure 13.**  $H_2$  permeability through various metals vs. temperature. With permission of reprint by Elsevier from [133].

### 3.2. Glycerol Steam Reforming in Conventional and Membrane Reactors

Most of the literature regarding the glycerol steam reforming reaction for producing hydrogen regards conventional reactors, both in aqueous or gas phase. When performed in gas phase, the process needs atmospheric pressure even though a consistent catalyst deactivation represents the most critical issue. Metals such as Ni and Ru exhibit good catalytic activity but lead to alkanes formation. In contrast, Ir, Co, Cu, Ag, Au and Fe show low catalytic activity. In literature, the catalytic activity scale for gas phase GSR reaction can be represented as in the following:  $Ru \approx Rh > Ni > Ir > Co > Pt > Pd > Fe$  [134]. Among the most active catalysts for this reaction, Rh results to be more effective to steam reforming of hydrocarbons and less susceptible to carbon formation, but Rh-based catalysts are not common in industrial applications owing to their high cost. Zhang et al. [135] performed both steam reforming reaction of ethanol and glycerol over Ir, Co and Ni-based catalysts, determining that Ir-based catalyst is significantly more active and selective toward hydrogen production. Iriondo et al. [136] used alumina-supported Ni-based catalysts, modified with Ce, Mg, Zr and La, pointing out that the differences in catalytic activity are due to the geometric effects caused by the Ni and La or to the close interaction between Ni and Zr. Furthermore, they found that the catalyst deactivation takes

place owing to the oxidation of the active catalyst metallic phase. The effect of the supports such as yttria, ceria-zirconia and  $\gamma$ -alumina on catalysts based on Ru and Ru-Me (with Me = Fe, Co, Ni, and Mo) was studied at high temperatures during glycerol steam reforming reaction [137]. It was found that the catalytic properties are notably affected by the nature of the support, resulting in a significant enhancement of H<sub>2</sub> production turnover rate and product selectivity on the reducible yttria and ceria-zirconia via facilitation of the water-gas shift reaction. The production of pure hydrogen from crude glycerol in a one-stage sorption enhanced steam reforming process (integrating steam reforming of oxygenates and hydrocarbons, WGS and carbonation reactions) was also studied by Feroso et al. [138]. In a CR packed with a mixture of Ni/Co catalyst derived from hydrotalcite-like material and dolomite as CO<sub>2</sub> sorbent, they reached an H<sub>2</sub> yield up to 88% and a hydrogen purity = 99.7 vol % at atmospheric pressure, temperature between 550 and 600 °C and WGMR = 3/1. Other interesting results are reported in a small overview on the most representative literature data about GSR reaction in CRs, in which the performance in terms of glycerol conversion are summarized in function on the reaction temperature and catalyst type used during the reaction (Table 6). As a qualitative comparison, Ru and Ni catalysts seem to have the best catalytic activity towards the reaction, favouring higher glycerol conversion.

**Table 6.** Glycerol conversion during GSR reaction in conventional and membrane reactors at various temperatures and catalysts.

Type of Reactor	Catalyst	T (°C)	Conversion (%)	Ref.
CR	Ni/Al <sub>2</sub> O <sub>3</sub>	635	100	Demsash & Mohan [139]
CR	Ni/ZrO <sub>2</sub>	600	100	Iriondo et al. [136]
CR	Ni/Al <sub>2</sub> O <sub>3</sub>	920	95	Adikari et al. [141]
CR	Ni/CrO <sub>2</sub>	400	100	Chen et al. [143]
CR	Ni/CeO <sub>2</sub> /Al <sub>2</sub> O <sub>3</sub>	600	92	Buffoni et al. [142]
CR	Rh/CeO <sub>2</sub> /Al <sub>2</sub> O <sub>3</sub>	920	78	Adikari et al. [141]
CR	Pt/CeZrO <sub>2</sub> /Y <sub>2</sub> O <sub>3</sub>	600	81	Cui et al. [143]
CR	Co/Al <sub>2</sub> O <sub>3</sub>	550	65	Cheng et al. [94]
CR	Rh/Al <sub>2</sub> O <sub>3</sub>	630	85	Chiodo et al. [146]
CR	Ru/Al <sub>2</sub> O <sub>3</sub>	720	100	Byrd et al. [147]
CR	Ni/CeO <sub>2</sub> /Al <sub>2</sub> O <sub>3</sub>	800	96	Lin et al. [148]
CR	Ni/Cu/Al	650	91	Wang et al. [149]
CR	Co/Al <sub>2</sub> O <sub>3</sub>	400	40	Iulianelli et al. [150]
CR	Ru/Al <sub>2</sub> O <sub>3</sub>	400	45	Iulianelli et al. [151]
Pd-Ag/PSS MR	Ni/CeO <sub>2</sub> /Al <sub>2</sub> O <sub>3</sub>	450	27	Lin et al. [148]
Pd-Ag MR	Co/Al <sub>2</sub> O <sub>3</sub>	400	94	Iulianelli et al. [150]
Pd-Ag MR	Ru/Al <sub>2</sub> O <sub>3</sub>	400	57	Iulianelli et al. [151]
Pd-Ag/PSS MR	Ni/CeO <sub>2</sub> /Al <sub>2</sub> O <sub>3</sub>	400	24	Chang et al. [153]
Pd-Ag/PSS MR	Ni/CeO <sub>2</sub> /Al <sub>2</sub> O <sub>3</sub>	450	95	Lin et al. [154]

As an alternative technology, a few authors investigated GSR reaction in membrane reactors and some results are also reported in Table 6. In particular, the main indication given by this table is that Pd-based MRs can operate at lower temperature than the CRs, meanwhile reaching comparable or better glycerol conversions. This represents an important goal because lower operating temperatures mean higher energy saving and, consequently, cheaper solution for performing the GSR reaction than the conventional processes, with the further advantage of collecting high grade hydrogen. As a special extension of the results related to MRs, Table 7 summarizes other performance in terms of both hydrogen recovery and yield besides other information regarding the operation conditions and the thickness of the dense Pd or Pd-alloy layer.

**Table 7.** Experimental data from literature about glycerol reforming in membrane reactors.

Type of Reactor	Pd or Pd-Alloy Layer	<i>T</i> (°C)	<i>p</i> (bar)	H <sub>2</sub> Recovery <sup>(a)</sup>	H <sub>2</sub> Yield <sup>(b)</sup>	Ref.
Pd-Ag/PSS	33	450	–	–	35	Lin et al. [148]
Pd-Ag MR	50	400	1.0	63	39	Iulianelli et al. [150]
Pd-Ag MR	50	400	5.0	56	28	Iulianelli et al. [151]
Pd-Ag/PSS	25	450	3	40	80	Chang et al. [153]
Pd-Ag/PSS	27	4	1	–	44	Lin et al. [154]

<sup>(a)</sup> H<sub>2</sub> Recovery = Molar ratio between the CO<sub>x</sub>-free hydrogen permeated stream and the total hydrogen really produced. <sup>(b)</sup> H<sub>2</sub> Yield = Molar ratio between the hydrogen stream in the permeate side and the total hydrogen theoretically producible from the stoichiometry of reaction.

Lin et al. [148] studied the autothermal glycerol reforming over a Ni/CeO<sub>2</sub>/Al<sub>2</sub>O<sub>3</sub> catalyst in a MR housing a Pd-Ag/PSS (thickness of the Pd-Ag layer = 33 μm). At 450 °C and WGMR = 5/1, they reached a hydrogen yield of around 35%. In another work, Lin et al. [153] evaluated also the effect of the oxygen addition on the hydrogen yield, reaching a value of around 44%. Chang et al. [153] used a supported porous stainless steel with a Pd-Ag layer deposited via electroless plating (25 μm of dense layer). This membrane was allocated in a MR, which was operated at 450 °C, getting 40% of hydrogen recovery and around 80% of hydrogen yield. Iulianelli et al. [150] allocated a dense and self-supported Pd-Ag membrane (50 μm thick) in a MR module and GSR reaction was carried out over a 0.5 wt % Ru/Al<sub>2</sub>O<sub>3</sub> catalyst. The experiments were performed at 400 °C, WGMR = 6/1, reaction pressure between 1 and 5 bar and WHSV from 0.1 to 1.0 h<sup>-1</sup>. At 5 bar, around 40% of glycerol conversion was reached with an H<sub>2</sub> recovery a bit less than 60%. Furthermore, Iulianelli et al. [151] studied the reaction over a Co/Al<sub>2</sub>O<sub>3</sub> commercial catalyst at 400 °C, WGMR = 6/1, reaction pressure between 1 and 4 bar, producing a maximum glycerol conversion around 94% and an H<sub>2</sub> recovery a bit higher than 60%.

#### 4. Conclusions

Glycerol production can come from different processes and feedstocks, such as by propylene synthesis via several pathways or hydrolysis of fatty acids triglycerides or by transesterification of fatty acids/oils. Furthermore, glycerol can be also produced via fermentation. However, among other renewable and bio-derived sources, glycerol has become an attracting candidate since it constitutes a relevant and alternative solution to produce hydrogen through reforming reactions, performed both in conventional and innovative reactors. In this section, we described the most common processes for obtaining glycerol. Also the role of the catalysts in the reforming reactions of glycerol to produce hydrogen has been considered because demonstrated that the steam reforming performances are much affected by the nature and composition of the catalysts used in the process. Furthermore, as a special case, we illustrated the main benefits of the utilization of an alternative and innovative technology as the membrane reactors in the field of hydrogen production. Indeed, we highlighted that Pd-based MR technology can show superior performance over the conventional reactors, or—in contrast—the same performances but operating at milder conditions, with a consequent advantage in terms of energy saving coupled to the recovery of an high-grade hydrogen stream. In summary, the future perspectives on performing the glycerol reforming in inorganic MRs are listed below:

- The scaling-up of glycerol reforming MRs is one of the most important issues. Developing low-cost, durable and defect-free membranes could represent a viable solution for realistic application of MRs at industrial scale.
- Great attention should be paid to evaluating the effective balance between benefits and drawbacks of applying MR technology to produce hydrogen from glycerol reforming reaction over the conventional processes.
- More wider researches on the lifetime of MRs utilized for carrying out glycerol reforming processes should be undertaken in order to validate them as a potential and alternative solution to the conventional systems at larger scales.

**Acknowledgments:** The Authors are grateful to Simona Liguori for the English editing of the manuscript.

**Author Contributions:** Giuseppe Bagnato wrote the paper for what concerns the glycerol production; Adolfo Iulianelli partially wrote the paper for what concerns membrane technology applied to glycerol exploitation, Aimaro Sanna edited the whole paper and Angelo Basile participated to the preparation of the whole paper.

**Conflicts of Interest:** The authors declare no conflict of interest.

### List of Acronyms and Symbol

BCC	Body centered cubic
$d_{pore}$	Pore diameter
$E_a$	Activation energy
$f_i^o$	Fugacity for $i$ -component
FCC	Face centered cubic
FFA	Free fatty acid
G	Free Gibbs energy
GOSR	Glycerol oxidative steam reforming
GSR	Glycerol steam reforming
$J_{H_2}$	Hydrogen flux through the membrane
$K$	Equilibrium constant
$k_i$	Kinetic constant for $i$ -reaction
LTA	Linde-type 5A zeolite
MONG	Matter organic non-glycerol
MR	Membrane reactor
MW	Molecular weight
OGMR	Oxygen glycerol molar ratio
P	Pressure
$p_{H_2,ret}$	Hydrogen partial pressure in the retentate side
$p_{H_2,perm}$	Hydrogen partial pressure in the permeate side
$P_{eH_2}$	Hydrogen permeability through the membrane
$P_{eH_2}^o$	Pre-exponential factor
R	Universal ideal gas constant
S	Entropy
SRM	Steam reforming of methane
T	Temperature
TR	Traditional reactor
WGS	Water gas shift
WGMR	Water glycerol molar ratio
WHSV	Weight hourly space velocity
$\delta$	Palladium thickness
$\varepsilon$	Membrane void fraction
$\tau$	Tortuosity
$\nabla p$	Pressure gradient
$\eta$	Viscosity
$\nu_i$	Stoichiometric coefficient for $i$ -component

### References

1. Ciriminna, R.; Pina, C.D.; Rossi, M.; Pagliaro, M. Understanding the glycerol market. *Eur. J. Lipid Sci. Technol.* **2014**, *116*, 1432–1439.
2. Stelmachowski, M. Utilization of glycerol, a by-product of the transesterification process of vegetable oils: A review. *Ecol. Chem. Eng.* **2011**, *18*, 9–30.
3. Speight, J.G. *Chemical and Process Design Handbook*; The McGraw-Hill Comp. Inc.: New York, NY, USA, 2002; ISBN: 0-07-137433-7.



4. Anitha, M.; Kamarudin, S.K.; Kofli, N.T. The potential of glycerol as a value-added commodity. *Chem. Eng. J.* **2016**, *295*, 119–130.
5. Formo, M.W. Physical properties of fats and fatty acids. In *Bailey's Industrial Oil and Fat Products*, 4th ed.; John Wiley and Sons: New York, NY, USA, 1979; Volume 1.
6. Bagheri, S.; Julkapli, N.M.; Yehye, W.A. Catalytic conversion of biodiesel derived raw glycerol to value added products. *Renew. Sustain. Energy Rev.* **2015**, *41*, 113–127. [[CrossRef](#)]
7. Annie, D. *Biofuels Production, Trade and Sustainable Development: Emerging Issues*; Environmental Economics Programme/Sustainable Markets Group: London, UK, 2006.
8. Shukla, K.; Srivastava, V.C. Synthesis of organic carbonates from alcoholysis of urea: A review. *Catal. Rev. Sci. Eng.* **2017**, *59*, 1–43.
9. Manosak, R.; Limpattayanate, H.S. Sequential-refining of crude glycerol derived from waste used-oil methyl ester plant via a combined process of chemical and adsorption. *Fuel Process. Technol.* **2001**, *92*, 92–99.
10. Matar, S.; Hatch, L.F. *Chemistry of Petrochemical Processes*, 2nd ed.; Gulf Publishing Company: Houston, TX, USA, 2000.
11. Hunt, J.A. A short history of soap. *Pharm. J.* **1999**, *263*, 985–899.
12. Marchetti, J.M.; Miguel, V.U.; Errazu, A.F. Possible methods for biodiesel production. *Renew. Sustain. Energy Rev.* **2007**, *11*, 1300–1311.
13. Quispe, C.A.G.; Coronado, C.J.R.; Carvalho, J.A., Jr. Glycerol: Production, consumption, prices, characterization and new trends in combustion. *Renew. Sustain. Energy Rev.* **2013**, *27*, 475–493. [[CrossRef](#)]
14. Wang, Z.X.; Zhuge, J.; Fang, H.; Prior, B.A. Glycerol production by microbial fermentation: A review. *Biotechnol. Adv.* **2001**, *19*, 201–223. [[PubMed](#)]
15. Fukuda, H.; Kond, A.; Noda, H. Biodiesel fuel production by transesterification of oils. *J. Biosci. Bioeng.* **2001**, *92*, 405–416. [[PubMed](#)]
16. Bournay, L.; Casanave, D.; Delfort, B.; Hillion, G.; Chodorge, J.A. New heterogeneous process for bio diesel production: A way to improve the quality and the value of the crude glycerin produced by biodiesel plants. *Catal. Today* **2005**, *106*, 190–192.
17. Ilham, Z.; Saka, S. Dimethyl carbonate as potential reactant in non-catalytic biodiesel production by supercritical method. *Bioresour. Technol.* **2009**, *100*, 1793–1796. [[CrossRef](#)] [[PubMed](#)]
18. Goembira, F.; Saka, S. Optimization of biodiesel production by supercritical methyl acetate. *Bioresour. Technol.* **2013**, *131*, 47–52. [[PubMed](#)]
19. Saka, S.; Isayama, Y.; Ilham, Z.; Jiayu, X. New process for catalyst-free biodiesel production using subcritical acetic acid and supercritical methanol. *Fuel* **2010**, *89*, 1442–1446.
20. Lam, M.K.; Lee, K.T.; Mohamed, A.R. Homogeneous, heterogeneous and enzymatic catalysis for transesterification of high free fatty acid oil (waste cooking oil) to biodiesel: A review. *Biotechnol. Adv.* **2010**, *28*, 500–518. [[CrossRef](#)] [[PubMed](#)]
21. Hidawati, E.N.; Mimi Sakinah, A.M. Treatment of Glycerin Pitch from Biodiesel Production. *Int. J. Chem. Environ. Eng.* **2011**, *5*, 309–313.
22. Hiremath, A.; Kannabiran, M.; Rangaswamy, V. 1,3-Propanediol production, from crude glycerol from jatropha biodiesel process. *New Biotechnol.* **2011**, *28*, 19–23. [[CrossRef](#)] [[PubMed](#)]
23. Hu, S.; Luo, X.; Wan, C.; Li, Y. Characterization of crude glycerol from biodiesel plants. *J. Agric. Food Chem.* **2012**, *60*, 5915–5921. [[CrossRef](#)] [[PubMed](#)]
24. Liu, Y.-P.; Sun, Y.; Tan, C.; Li, H.; Zheng, X.J.; Jin, K.Q.; Wang, G. Efficient production of dihydroxyacetone from biodiesel-derived crude glycerol by newly isolated *Gluconobacter frateurii*. *Bioresour. Technol.* **2013**, *142*, 384–389. [[PubMed](#)]
25. Tan, H.W.; Aziz, A.A.; Aroua, M.K. Glycerol production and its applications as a raw material: A review. *Renew. Sustain. Energy Rev.* **2013**, *27*, 118–127. [[CrossRef](#)]
26. Bouaid, A.; Vázquez, R.; Martínez, M.; Aracil, J. Effect of free fatty acids contents on biodiesel quality. Pilot plant studies. *Fuel* **2016**, *174*, 54–62. [[CrossRef](#)]
27. Zheng, Y.; Chen, X.; Shen, Y. Commodity Chemicals Derived from Glycerol, an Important Biorefinery Feedstock. *Chem. Rev.* **2008**, *108*, 5253–5277. [[PubMed](#)]
28. Luo, X.; Ge, X.; Cui, S.; Li, Y. Value-added processing of crude glycerol into chemicals and polymers. *Rev. Bioresour. Technol.* **2016**, *215*, 144–154.



29. Almeida, J.R.M.; Fávaro, L.C.L.; Quirino, B.F. Biodiesel biorefinery: Opportunities and challenges for microbial production of fuels and chemicals from glycerol waste. *Biotechnol. Biofuels* **2012**, *5*, 48. [[CrossRef](#)]
30. Hirasawa, S.; Watanabe, H.; Kizuka, T.; Nakagawa, Y.; Tomishige, K. Performance, structure and mechanism of Pd–Ag alloy catalyst for selective oxidation of glycerol to dihydroxyacetone. *J. Catal.* **2013**, *300*, 205–216.
31. Ning, X.; Li, Y.; Yu, H.; Peng, F.; Wang, H.; Yang, Y. Promoting role of bismuth and antimony on Pt catalysts for the selective oxidation of glycerol to dihydroxyacetone. *J. Catal.* **2016**, *335*, 95–104.
32. Rodrigues, E.G.; Pereira, M.F.R.; Delgado, J.J.; Chen, X.; Órfão, J.J.M. Enhancement of the selectivity to dihydroxyacetone in glycerol oxidation using gold nanoparticles supported on carbon nanotubes. *Catal. Commun.* **2011**, *16*, 64–69.
33. Li, Y.; Zaera, F. Sensitivity of the glycerol oxidation reaction to the size and shape of the platinum nanoparticles in Pt/SiO<sub>2</sub> catalysts. *J. Catal.* **2015**, *326*, 116–126.
34. Wang, F.F.; Shao, S.; Liu, C.L.; Xu, C.L.; Yang, R.Z.; Dong, W.S. Selective oxidation of glycerol over Pt supported on mesoporous carbon nitride in base-free aqueous solution. *Chem. Eng. J.* **2015**, *264*, 336–343.
35. Olmos, C.M.; Chinchilla, L.E.; Rodrigues, E.G.; Delgado, J.J.; Hungria, A.B.; Blanco, G.; Pereira, M.F.R.; Órfão, J.J.M.; Calvino, J.J.; Chen, X. Synergistic effect of bimetallic Au–Pd supported on ceria-zirconia mixed oxide catalysts for selective oxidation of glycerol. *Appl. Catal. B Environ.* **2016**. [[CrossRef](#)]
36. Skrzynska, E.; Zaid, S.; Girardon, J.S.; Capron, M.; Dumeignil, F. Catalytic behaviour of four different supported noble metals in the crude glycerol oxidation. *Appl. Catal. A Gen.* **2015**, *499*, 89–100.
37. Gil, S.; Marchena, M.; Fernández, C.M.; Sánchez-Silva, L.; Romero, A.; Valverde, J.L. Catalytic oxidation of crude glycerol using catalysts based on Au supported on carbonaceous materials. *Appl. Catal. A Gen.* **2013**, *450*, 189–203.
38. Xu, C.; Du, Y.; Li, C.; Yang, J.; Yang, G. Insight into effect of acid/base nature of supports on selectivity of glycerol oxidation over supported Au–Pt bimetallic catalysts. *Appl. Catal. B Environ.* **2015**, *164*, 334–343.
39. Fordham, P.; Besson, M.; Gallezot, P. Selective oxidation with air of glyceric to hydroxypyruvic acid and tartronic to mesoxalic acid on PtBi/C catalysts. *Stud. Surf. Sci. Catal.* **1997**, *108*, 429–436.
40. Lee, S.H.; Moon, D.J. Studies on the conversion of glycerol to 1,2-propanediol over Ru-based catalyst under mild conditions. *Catal. Today* **2011**, *174*, 10–16.
41. Vasiliadou, E.S.; Heracleous, E.; Vasalos, I.A.; Lemonidou, A.A. Ru-based catalysts for glycerol hydrogenolysis—Effect of support and metal precursor. *Appl. Catal. B Environ.* **2009**, *92*, 90–99.
42. Soares, A.V.H.; Salazar, J.B.; Falcone, D.D.; Vasconcellos, F.A.; Davis, R.J.; Passos, F.B. A study of glycerol hydrogenolysis over Ru–Cu/Al<sub>2</sub>O<sub>3</sub> and Ru–Cu/ZrO<sub>2</sub> Catalysts. *J. Mol. Catal. A Chem.* **2016**, *415*, 27–36.
43. Van Ryneveld, E.; Mahomed, A.S.; van Heerden, P.S.; Friedrich, H.B. Direct hydrogenolysis of highly concentrated glycerol solutions over supported Ru, Pd and Pt catalyst systems. *Catal. Lett.* **2011**, *141*, 958–967.
44. Liu, H.; Liang, S.; Jiang, T.; Han, B.; Zhou, Y. Hydrogenolysis of glycerol to 1,2-propanediol over Ru–Cu bimetallic catalysts supported on different supports. *CLEAN* **2012**, *40*, 318–324.
45. Jiang, T.; Zhou, Y.; Liang, S.; Liu, H.; Han, B. Hydrogenolysis of glycerol catalyzed by Ru–Cu bimetallic catalysts supported on clay with the aid of ionic liquids. *Green Chem.* **2009**, *11*, 1000–1006.
46. Estevez, R.; Lopez-Pedrajas, S.; Blanco-Bonilla, F.; Luna, D.; Bautista, F.M. Production of acrolein from glycerol in liquid phase on heterogeneous Catalysts. *Chem. Eng. J.* **2015**, *282*, 179–186.
47. Cecilia, J.A.; García-Sancho, C.; Mérida-Robles, J.M.; Santamaría-González, J.; Moreno-Tost, R.; Maireles-Torres, P. V and V–P containing Zr-SBA-15 catalysts for dehydration of glycerol to acrolein. *Catal. Today* **2015**, *254*, 43–52.
48. Vitiello, R.; Russo, V.; Turco, R.; Tesser, R.; Di Serio, M.; Santacesaria, E. Glycerol chlorination in a gas-liquid semibatch reactor: New catalysts for chlorohydrin production. *Chin. J. Catal.* **2014**, *35*, 663–669.
49. Hu, W.; Zhang, Y.; Huang, Y.; Wang, J.; Gao, J.; Xu, J. Selective esterification of glycerol with acetic acid to diacetin using antimony pentoxide as reusable catalyst. *J. Energy Chem.* **2015**, *24*, 632–636.
50. Yusoff, M.H.M.; Abdullah, A.Z. Catalytic behavior of sulfated zirconia supported on SBA-15 as catalyst in selective glycerol esterification with palmitic acid to monopalmitin. *J. Taiwan Inst. Chem. Eng.* **2016**, *60*, 199–204.
51. Gao, X.; Zhu, S.; Li, Y. Graphene oxide as a facile solid acid catalyst for the production of bioadditives from glycerol esterification. *Catal. Commun.* **2015**, *62*, 48–51. [[CrossRef](#)]

52. Ishak, Z.I.; Sairi, N.A.; Alias, Y.; Aroua, M.K.T.; Yusoff, R. Production of glycerol carbonate from glycerol with aid of ionic liquid as catalyst. *Chem. Eng. J.* **2016**, *297*, 128–138. [[CrossRef](#)]
53. Munshi, M.K.; Biradar, P.S.; Gade, S.M.; Rane, V.H.; Kelkar, A.A. Efficient synthesis of glycerol carbonate/glycidol using 1,8-diazabicyclo [5.4.0] undec-7-ene (DBU) based ionic liquids as catalyst. *RSC Adv.* **2014**, *4*, 17124–17128.
54. Liu, J.; Li, Y.; Zhang, J.; He, D. Glycerol carbonylation with CO<sub>2</sub> to glycerol carbonate over CeO<sub>2</sub> catalyst and the influence of CeO<sub>2</sub> preparation methods and reaction parameters. *Appl. Catal. A Gen.* **2016**, *513*, 9–18.
55. Fernandez, Y.; Arenillas, A.; Díez, M.A.; Pis, J.J.; Menendez, J.A. Pyrolysis of glycerol over activated carbons for syngas production. *J. Anal. Appl. Pyrolysis* **2009**, *84*, 145–150.
56. Liu, H.J.; Xu, Y.Z.; Zheng, Z.M.; Liu, D.H. 1,3-Propanediol and its copolymers: Research, development and industrialization. *Biotechnol. J.* **2010**, *5*, 1137–1148.
57. Johnson, E.E.; Rehmann, L. The role of 1,3-propanediol production in fermentation of glycerol by *Clostridium pasteurianum*. *Bioresour. Technol.* **2016**, *209*, 1–7. [[PubMed](#)]
58. Chen, X.; Zhang, D.J.; Qi, W.T.; Gao, S.J.; Xiu, Z.L.; Xu, P. Microbial fed-batch production of 1,3-propanediol by *Klebsiella pneumoniae* under micro-aerobic conditions. *Appl. Microbiol. Biotechnol.* **2003**, *63*, 143–146. [[PubMed](#)]
59. Xu, Y.Z.; Guo, N.N.; Zheng, Z.M.; Ou, X.J.; Liu, H.J.; Liu, D.H. Metabolism in 1,3-propanediol fed-batch fermentation by a D-lactate deficient mutant of *Klebsiella pneumoniae*. *Biotechnol. Bioeng.* **2009**, *104*, 965–972. [[CrossRef](#)]
60. Papanikolaou, S.; Fakas, S.; Fick, M.; Chevalot, I.; Galiotou-Panayotou, M.; Komaitis, M.; Marc, I.; Aggelis, G. Biotechnological valorisation of raw glycerol discharged after bio-diesel (fatty acid methyl esters) manufacturing process: Production of 1,3-propanediol, citric acid and single cell oil. *Biomass Bioenergy* **2008**, *32*, 60–71.
61. Tang, X.M.; Tan, Y.S.; Zhu, H.; Zhao, K.; Shen, W. Microbial Conversion of Glycerol to 1,3-Propanediol by an Engineered Strain of *Escherichia coli*. *Appl. Environ. Microb.* **2009**, *75*, 1628–1634.
62. Liu, H.J.; Zhang, D.J.; Xu, Y.H.; Mu, Y.; Sun, Y.Q.; Xiu, Z.L. Microbial production of 1,3-propanediol from glycerol by *Klebsiella pneumoniae* under micro-aerobic conditions up to a pilot scale. *Biotechnol. Lett.* **2007**, *29*, 1281–1285.
63. Petrov, K.; Petrova, P. High production of 2,3-butanediol from glycerol by *Klebsiella pneumoniae* G31. *Appl. Microbiol. Biotechnol.* **2009**, *84*, 659–665. [[CrossRef](#)] [[PubMed](#)]
64. Ji, X.J.; Huang, H.; Ouyang, P.K. Microbial 2,3-butanediol production: A state-of-the-art review. *Biotechnol. Adv.* **2011**, *29*, 351–364. [[PubMed](#)]
65. Petrov, K.; Petrova, P. Enhanced production of 2,3-butanediol from glycerol by forced pH fluctuations. *Appl. Microbiol. Biotechnol.* **2010**, *87*, 943–949.
66. Nitayavardhana, S.; Khanal, S.K. Innovative biorefinery concept for sugar-based ethanol industries: Production of protein-rich fungal biomass on vinasse as an aquaculture feed ingredient. *Bioresour. Technol.* **2010**, *101*, 9078–9085. [[PubMed](#)]
67. Durnin, G.; Clomburg, J.; Yeates, Z.; Alvarez, P.J.J.; Zygorakis, K.; Campbell, P.; Gonzalez, R. Understanding and Harnessing the Microaerobic Metabolism of Glycerol in *Escherichia coli*. *Biotechnol. Bioeng.* **2009**, *103*, 148–161. [[PubMed](#)]
68. Harvey, B.G.; Meylemans, H.A. The role of butanol in the development of sustainable fuel technologies. *J. Chem. Technol. Biotechnol.* **2011**, *86*, 2–9.
69. Taconi, K.A.; Venkataramanan, K.P.; Johnson, D.T. Growth and Solvent Production by *Clostridium pasteurianum* ATCC (R) 6013 (TM) Utilizing Biodiesel-Derived Crude Glycerol as the Sole Carbon Source. *Environ Prog. Sustain. Energy* **2009**, *28*, 100–110.
70. Sarchami, T.; Johnson, E.; Rehmann, L. Optimization of fermentation condition favoring butanol production from glycerol by *Clostridium pasteurianum* DSM 525. *Bioresour. Technol.* **2016**, *208*, 73–80. [[CrossRef](#)]
71. Petersen, A.B.; Na, R.; Wulf, H.C. Sunless skin tanning with dihydroxyacetone delays broad-spectrum ultraviolet photocarcinogenesis in hairless mice. *Mutat. Res.* **2003**, *542*, 129–138. [[PubMed](#)]
72. Hu, Z.C.; Liu, Z.Q.; Zheng, Y.G.; Shen, Y.C. Production of 1,3-Dihydroxyacetone from Glycerol by *Gluconobacter oxydans* ZJB09112. *J. Microbiol. Biotechnol.* **2010**, *20*, 340–345. [[PubMed](#)]
73. Habe, H.; Fukuoka, T.; Kitamoto, D.; Sakaki, K. Biotechnological production of D-glyceric acid and its application. *Appl. Microbiol. Biotechnol.* **2009**, *84*, 445–452.

74. Habe, H.; Shimada, Y.; Yakushi, T.; Hattori, H.; Ano, Y.; Fukuoka, T.; Kitamoto, D.; Itagaki, M.; Watanabe, K.; Yanagishita, H. Microbial Production of Glyceric Acid, an Organic Acid That Can Be Mass Produced from Glycerol. *Appl. Environ. Microbiol.* **2009**, *75*, 7760–7766. [[PubMed](#)]
75. Castro-Aguirre, E.; Iñiguez-Franco, F.; Samsudin, H.; Fang, X.; Auras, R. Poly(lactic acid)-Mass production, processing, industrial applications, and end of life. *Adv. Drug Deliv. Rev.* **2016**, *107*, 333–366. [[CrossRef](#)] [[PubMed](#)]
76. Hong, A.A.; Cheng, K.K.; Peng, F.; Zhou, S.; Sun, Y.; Liu, C.M.; Liu, D.H. Strain isolation and optimization of process parameters for bioconversion of glycerol to lactic acid. *J. Chem. Technol. Biotechnol.* **2009**, *84*, 1576–1581.
77. Mazumdar, S.; Clomburg, J.M.; Gonzalez, R. *Escherichia coli* strains engineered for homofermentative production of D-lactic acid from glycerol. *Appl. Environ. Microbiol.* **2010**, *76*, 4327–4336. [[PubMed](#)]
78. Harry-O'kurua, R.E.; Gordon, S.H.; Klokkenga, M. Bio-generation of succinic acid by fermentation of *Physaria fendleri* seed polysaccharides. *Ind. Crops Prod.* **2015**, *77*, 116–122.
79. Blankschien, M.D.; Clomburg, J.M.; Gonzalez, R. Metabolic engineering of *Escherichia coli* for the production of succinate from glycerol. *Metab. Eng.* **2010**, *12*, 409–419. [[PubMed](#)]
80. Yuzbashev, T.V.; Yuzbasheva, E.Y.; Sobolevskaya, T.I.; Laptev, I.A.; Vybornaya, T.V.; Larina, A.S.; Matsui, K.; Fukui, K.; Sineoky, S.P. Production of Succinic Acid at Low pH by a Recombinant Strain of the Aerobic Yeast *Yarrowia lipolytica*. *Biotechnol. Bioeng.* **2010**, *107*, 673–682.
81. Papanikolaou, S.; Muniglia, L.; Chevalot, I.; Aggelis, G.; Marc, I. *Yarrowia lipolytica* as a potential producer of citric acid from raw glycerol. *J. Appl. Microbiol.* **2002**, *92*, 737–744. [[PubMed](#)]
82. Rymowicz, W.; Fatykhova, A.R.; Kamzolova, S.V.; Rywinska, A.; Morgunov, I.G. Citric acid production from glycerol-containing waste of biodiesel industry by *Yarrowia lipolytica* in batch, repeated batch, and cell recycle regimes. *Appl. Microbiol. Biotechnol.* **2010**, *87*, 971–979. [[PubMed](#)]
83. Musial, I.; Cibis, E.; Rymowicz, W. Designing a process of kaolin bleaching in an oxalic acid enriched medium by *Aspergillus niger* cultivated on biodiesel-derived waste composed of glycerol and fatty acids. *Appl. Clay Sci.* **2011**, *52*, 277–284.
84. Andre, A.; Diamantopoulou, P.; Philippoussis, A.; Sarris, D.; Komaitis, M.; Papanikolaou, S. Biotechnological conversions of bio-diesel derived waste glycerol into added-value compounds by higher fungi: Production of biomass, single cell oil and oxalic acid. *Ind. Crop. Prod.* **2010**, *31*, 407–416.
85. Li, H.; Ding, X.; Zhao, Y.C.; Han, B.H. Preparation of mannitol-based ketal-linked porous organic polymers and their application for selective capture of carbon dioxide. *Polymer* **2016**, *89*, 112–118.
86. Khan, A.; Bhide, A.; Gadre, R. Mannitol production from glycerol by resting cells of *Candida magnolia*. *Bioresour. Technol.* **2009**, *100*, 4911–4913. [[PubMed](#)]
87. Saran, S.; Mukherjee, S.; Dalal, J.; Saxena, R.K. High production of erythritol from *Candida sorbosivorans* SSE-24 and its inhibitory effect on biofilm formation of *Streptococcus mutans*. *Bioresour. Technol.* **2015**, *198*, 31–38. [[CrossRef](#)] [[PubMed](#)]
88. Rymowicz, W.; Rywinska, A.; Marcinkiewicz, M. High-yield production of erythritol from raw glycerol in fed-batch cultures of *Yarrowia lipolytica*. *Biotechnol. Lett.* **2009**, *31*, 377–380.
89. Koganti, S.; Kuo, T.M.; Kurtzman, C.P.; Smith, N.; Ju, L.K. Production of arabitol from glycerol: Strain screening and study of factors affecting production yield. *Appl. Microbiol. Biotechnol.* **2011**, *90*, 257–267. [[PubMed](#)]
90. Prabisha, T.P.; Sindhua, R.; Binoda, P.; Sankar, V.; Raghu, K.G.; Pandey, A. Production and characterization of PHB from a novel isolate *Comamonas* sp. from a dairy effluent sample and its application in cell culture. *Biochem. Eng. J.* **2015**, *101*, 150–159. [[CrossRef](#)]
91. Nickel, P.I.; Pettinari, M.J.; Galvagno, M.A.; Mendez, B.S. Poly(3-hydroxybutyrate) synthesis from glycerol by a recombinant *Escherichia coli* arca mutant in fed-batch microaerobic cultures. *Appl. Microbiol. Biotechnol.* **2008**, *77*, 1337–1343. [[CrossRef](#)]
92. Ibrahim, M.H.A.; Steinbuchel, A. Poly(3-Hydroxybutyrate) Production from Glycerol by *Zobellella denitrificans* MW1 via High-Cell-Density Fed-Batch Fermentation and Simplified Solvent Extraction. *Appl. Environ. Microbiol.* **2009**, *75*, 6222–6231. [[CrossRef](#)] [[PubMed](#)]
93. Sutar, P.N.; Vaidya, P.D.; Rodrigues, A.E. Glycerol-reforming kinetics using a Pt/C catalyst. *Chem. Eng. Technol.* **2010**, *33*, 1645–1649.

94. Cheng, C.K.; Foo, S.Y.; Adesina, A.A. H<sub>2</sub>-rich synthesis gas production over Co/Al<sub>2</sub>O<sub>3</sub> catalyst via glycerol steam reforming. *Catal. Commun.* **2010**, *12*, 292–298. [[CrossRef](#)]
95. Cheng, C.K.; Foo, S.Y.; Adesina, A.A. Steam reforming of glycerol over Ni/Al<sub>2</sub>O<sub>3</sub> catalyst. *Catal. Today* **2011**, *178*, 25–33.
96. Cheng, C.K.; Foo, S.Y.; Adesina, A.A. Glycerol steam reforming over bimetallic Co-Ni/Al<sub>2</sub>O<sub>3</sub>. *Ind. Eng. Chem. Res.* **2010**, *49*, 10804–10817. [[CrossRef](#)]
97. Adhikari, S.; Fernando, S.; Haryanto, A. Kinetics and reactor modeling of hydrogen production from glycerol via steam reforming process over Ni/CeO<sub>2</sub> catalysts. *Chem. Eng. Technol.* **2009**, *32*, 541–547. [[CrossRef](#)]
98. Dave, C.D.; Pant, K.K. Renewable hydrogen generation by steam reforming of glycerol over zirconia promoted ceria supported catalyst. *Renew. Energy* **2011**, *36*, 3195–3202. [[CrossRef](#)]
99. Calles, J.A.; Carrero, A.; Vizcaíno, A.J.; Moreno, L.G. Hydrogen production by glycerol steam reforming over SBA-15-supported nickel catalysts: Effect of alkaline earth promoters on activity and stability. *Catal. Today* **2014**, *227*, 198–206.
100. Wang, C.; Dou, B.; Chen, H.; Song, Y.; Xu, Y.; Du, X.; Luo, T.; Tan, C. Hydrogen production from steam reforming of glycerol by Ni-Mg-Al based catalysts in a fixed-bed reactor. *Chem. Eng. J.* **2013**, *220*, 133–142. [[CrossRef](#)]
101. Dieuzeide, M.L.; Iannibelli, V.; Jobbagy, M.; Amadeo, N. Steam reforming of glycerol over Ni/Mg/γ-Al<sub>2</sub>O<sub>3</sub> catalysts. Effect of calcination temperatures. *Int. J. Hydrogen Energy* **2012**, *37*, 14926–14930. [[CrossRef](#)]
102. Dieuzeide, M.L.; Laborde, M.; Amadeo, N.; Cannilla, C.; Bonura, G.; Frusteri, F. Hydrogen production by glycerol steam reforming: How Mg doping affects the catalytic behaviour of Ni/Al<sub>2</sub>O<sub>3</sub> catalysts. *Int. J. Hydrogen Energy* **2016**, *41*, 157–166. [[CrossRef](#)]
103. Seung-hoon, K.; Jae-sun, J.; Eun-hyeok, Y.; Kwan-Young, L.; Ju, M.D. Hydrogen production by steam reforming of biomass-derived glycerol over Ni-based catalysts. *Catal. Today* **2014**, *228*, 145–151. [[CrossRef](#)]
104. Huang, Z.Y.; Xu, C.H.; Meng, J.; Zheng, C.F.; Xiao, H.W.; Chen, J.; Zhang, Y.X. Glycerol steam reforming to syngas over Ni-based catalysts on commercial Linde-type 5A zeolite modified by metal oxides. *J. Environ. Chem. Eng.* **2014**, *2*, 598–604. [[CrossRef](#)]
105. Gallegos-Suárez, E.; García-García, F.R.; González-Jiménez, I.D.; Rodríguez-Ramos, I.; Guerreiro-Ruiz, A.; Li, K. Ceramic hollow fibres catalytic enhanced reactors for glycerol steam reforming. *Catal. Today* **2014**, *233*, 21–30. [[CrossRef](#)]
106. Shao, S.; Shi, A.W.; Liu, C.L.; Yang, R.Z.; Dong, W.S. Hydrogen production from steam reforming of glycerol over Ni/CeZrO catalysts. *Fuel Process. Technol.* **2014**, *125*, 1–7. [[CrossRef](#)]
107. Kousi, K.; Chourdakis, N.; Matralis, H.; Kontarides, D.; Papadopoulou, C.; Verykios, X. Glycerol steam reforming over modified Ni-based catalysts. *Appl. Catal. A Gen.* **2016**. [[CrossRef](#)]
108. Bobadilla, L.F.; Penkova, A.; Álvarez, A.; Domínguez, M.I.; Romero-Sarria, F.; Centeno, M.A.; Odriozola, J.A. Glycerol steam reforming on bimetallic NiSn/CeO<sub>2</sub>-MgO-Al<sub>2</sub>O<sub>3</sub> catalysts: Influence of the support, reaction parameters and deactivation/regeneration processes. *Appl. Catal. A Gen.* **2015**, *492*, 38–47. [[CrossRef](#)]
109. Go, Y.J.; Go, G.S.; Lee, H.J.; Moon, D.J.; Park, N.C.; Kim, Y.C. The relation between carbon deposition and hydrogen production in glycerol steam reforming. *Int. J. Hydrogen Energy* **2015**, *40*, 11840–11847.
110. Yurdakul, M.; Ayas, N.; Bizkarra, K.; El Doukkali, M.; Cambra, J.F. Preparation of Ni-based catalysts to produce hydrogen from glycerol by steam reforming process. *Int. J. Hydrogen Energy* **2016**, *41*, 8084–8091. [[CrossRef](#)]
111. Sundari, R.; Vaidya, P.D. Reaction Kinetics of Glycerol Steam Reforming Using a Ru/Al<sub>2</sub>O<sub>3</sub>. *Catal. Energy Fuels* **2012**, *26*, 4195–4204.
112. Hirai, T.; Ikenaga, N.; Miyake, T.; Suzuki, T. Production of Hydrogen by Steam Reforming of Glycerin on Ruthenium Catalyst. *Energy Fuels* **2005**, *19*, 1761–1762.
113. Sanchez, E.A.; Comelli, R.A. Hydrogen production by glycerol steam-reforming over nickel and nickel-cobalt impregnated on alumina. *Int. J. Hydrogen Energy* **2014**, *39*, 8650–8655.
114. Araque, M.; Martínez, L.M.T.; Vargas, J.C.; Centeno, M.A.; Roger, A.C. Effect of the active metals on the selective H<sub>2</sub> production in glycerol steam reforming. *Appl. Catal. B Environ.* **2012**, *125*, 556–566. [[CrossRef](#)]
115. Pompeo, F.; Santori, G.; Nichio, N.N. Hydrogen and/or syngas from steam reforming of glycerol. Study of platinum catalysts. *Int. J. Hydrogen Energy* **2010**, *35*, 8912–8920. [[CrossRef](#)]
116. Pompeo, F.; Santori, G.F.; Nichio, N.N. Hydrogen production by glycerol steam reforming with Pt/SiO<sub>2</sub> and Ni/SiO<sub>2</sub> Catalysts. *Catal. Today* **2011**, *172*, 183–188. [[CrossRef](#)]



117. Pastor-Pérez, L.; Merlo, A.; Buitrago-Sierra, R.; Casella, M.; Sepúlveda-Escribano, A. Document Bimetallic PtSn/C catalysts obtained via SOMC/M for glycerol steam reforming. *J. Colloid Interface Sci.* **2015**, *459*, 160–166. [[CrossRef](#)]
118. Sad, M.E.; Duarte, H.A.; Vignatti, C.; Padrò, C.L.; Apestegui, C.R. Steam reforming of glycerol: Hydrogen production optimization. *Int. J. Hydrogen Energy* **2015**, *40*, 6097–6106.
119. Surendar, M.; Sagar, T.V.; Raveendra, G.; Kumar, M.A.; Lingaiah, N.; Rao, K.R.; Prasad, P.S. Pt doped LaCoO<sub>3</sub> perovskite: A precursor for a highly efficient catalyst for hydrogen production from glycerol. *Int. J. Hydrogen Energy* **2016**, *41*, 2285–2297.
120. Ramesh, S.; Yang, E.H.; Jung, J.S.; Moon, D.J. Copper decorated perovskite an efficient catalyst for low temperature hydrogen production by steam reforming of glycerol. *Int. J. Hydrogen Energy* **2015**, *40*, 11428–11435. [[CrossRef](#)]
121. Mitran, G.; Pavel, O.D.; Florea, M.; Mieritz, D.G.; Seo, D.K. Hydrogen production from glycerol steam reforming over molybdena–alumina catalysts. *Catal. Commun.* **2016**, *77*, 83–88.
122. Iulianelli, A.; Dalena, F.; Liguori, S.; Calabrò, V.; Basile, A. Membrane reactors for steam reforming of glycerol and acetic acid. In *Membrane Reactors for Energy Applications AND Basic Chemical Production*; Basile, A., Hai, F., Di Paola, L., Piemonte, V., Eds.; Woodhead: Amsterdam, NL, USA, 2015; Chapter 8; pp. 249–266.
123. Basile, A.; Iulianelli, A.; Liguori, S. Membrane reactor: An integrated “membrane + reaction” system. In *Integrated Membrane Systems and Processes*; Basile, A., Charcosset, C., Eds.; John Wiley & Sons Ltd.: Hoboken, NJ, USA, 2016; Chapter 9; pp. 231–253, ISBN: 978-1-118-73908-2.
124. Iulianelli, A.; Liguori, S.; Wilcox, J.; Basile, A. Advances on methane steam reforming to produce hydrogen through membrane reactors technology: A review. *Catal. Rev. Sci. Eng.* **2016**, *58*, 1–35. [[CrossRef](#)]
125. Iulianelli, A.; Liguori, S.; Longo, T.; Basile, A. Inorganic membrane and membrane reactor technologies for hydrogen production. In *Hydrogen Production: Prospects and Processes*; Honery, D.R., Moriarty, P., Eds.; Series: Energy Science, Engineering and Technology; Nova Science Publishers: Victoria, Australia, 2012; Chapter 12; pp. 377–398, ISBN: 978-1-62100-246-8.
126. Briceño, K.; Iulianelli, A.; Montané, D.; Garcia-Valls, R.; Basile, A. Carbon molecular sieve membranes supported on non-modified ceramic tubes for hydrogen separation in membrane reactors. *Int. J. Hydrogen Energy* **2012**, *37*, 13536–13544.
127. Iulianelli, A.; Basile, A. Hydrogen production from ethanol via inorganic membrane reactors technology: A review. *Catal. Sci. Technol.* **2011**, *1*, 366–379. [[CrossRef](#)]
128. Basile, A.; Iulianelli, A.; Tong, J. Single-stage hydrogen production and separation from fossil fuels using micro- and macromembrane reactors. In *Compendium of Hydrogen Energy, Hydrogen Production and Purification*; Subramani, V., Basile, A., Veziroglu, T.N., Eds.; Series in Energy: Number 83; Woodhead Publishing: Amsterdam, NL, USA, 2015; Chapter 15; Volume 1, pp. 445–468.
129. Basile, A.; Iulianelli, A.; Longo, T.; Liguori, S.; De Falco, M. Pd-based Selective Membrane State-of-the-Art. In *Membrane Reactors for Hydrogen Production Processes*; De Falco, L.M.M., Iaquaniello, G., Eds.; Springer: London, UK; Dordrecht, The Netherlands; Heidelberg, Germany; New York, NY, USA, 2011; Chapter 2; pp. 21–55, ISBN: 978-0-85729-150-9.
130. Liguori, S.; Iulianelli, A.; Dalena, F.; Pinacci, P.; Drago, F.; Broglia, M.; Huang, Y.; Basile, A. Performance and long-term stability of Pd/PSS and Pd/Al<sub>2</sub>O<sub>3</sub> for hydrogen separation. *Membranes* **2014**, *4*, 143–162. [[CrossRef](#)]
131. Iulianelli, A.; Alavi, M.; Bagnato, G.; Liguori, S.; Wilcox, J.; Rahimpour, M.R.; Eslamlouyan, R.; Anzelmo, B.; Basile, A. Supported Pd-Au membrane reactor for hydrogen production: Membrane preparation, characterization and testing. *Molecules* **2016**, *21*, 581–594.
132. Iulianelli, A.; Liguori, S.; Morrone, P.; Basile, A. Membrane and membrane reactor technologies for CO<sub>x</sub> purification of gaseous streams. In *Advances in Chemistry Research*; Taylor, J.C., Ed.; Nova Science Publishers: New York, NY, USA, 2012; Volume 16, ISBN: 978-1-62081-395-9.
133. Al-Mufachi, N.A.; Rees, N.V.; Steinberger-Wilkens, R. Hydrogen selective membranes: A review of palladium-based dense metal membranes. *Renew. Sustain. Environ. Rev.* **2015**, *47*, 540–551.
134. Gallegos-Suárez, E.; Guerrero-Ruiz, A.; Rodríguez-Ramos, I. Efficient hydrogen production from glycerol by steam reforming with carbon supported ruthenium catalysts. *Carbon* **2016**, *96*, 578–587. [[CrossRef](#)]
135. Zhang, B.; Tang, X.; Li, Y.; Xu, Y.; Shen, W. Hydrogen production from steam reforming of ethanol and glycerol over ceria-supported metal catalysts. *Int. J. Hydrogen Environ.* **2007**, *32*, 2367–2373.

136. Iriondo, A.; Barrio, V.L.; Cambra, J.F.; Arias, P.L.; Guëmez, M.B.; Navarro, R.M.; Sánchez-Sánchez, M.C.; Fierro, J.L.G. Hydrogen production from glycerol over nickel catalysts supported on Al<sub>2</sub>O<sub>3</sub> modified by Mg, Zr, Ce or La. *Top. Catal.* **2008**, *49*, 46–58. [[CrossRef](#)]
137. Kim, J.; Lee, D. Glycerol steam reforming on supported Ru-based catalysts for hydrogen production for fuel cells. *Int. J. Hydrogen Environ.* **2013**, *38*, 11853–11862. [[CrossRef](#)]
138. Feroso, J.; He, L.; Chen, D. Production of high purity hydrogen by sorption enhanced steam reforming of crude glycerol. *Int. J. Hydrogen Environ.* **2012**, *37*, 14047–14054.
139. Demasash, H.D.; Mohan, R. Steam reforming of glycerol to hydrogen over ceria promoted nickel alumina catalysts. *Int. J. Hydrogen Energy* **2016**, *41*, 22732–22742. [[CrossRef](#)]
140. Kim, T.; Park, D. Preparation and characterization of Ni nanostructures coated on the substrates for glycerol steam reforming. *J. Nanosci. Nanotechnol.* **2017**, *17*, 2478–2481.
141. Adhikari, S.; Fernando, S.; Haryanto, A. Production of hydrogen by SR of glycerin over alumina-supported metal catalyst. *Catal. Today* **2007**, *129*, 355–364. [[CrossRef](#)]
142. Buffoni, I.N.; Pompeo, F.; Santori, G.F.; Nichio, N.N. Nickel catalysts applied in steam reforming of glycerol for hydrogen production. *Catal. Commun.* **2009**, *10*, 1656–1660. [[CrossRef](#)]
143. Cui, Y.; Galvita, V.; Rihko-Struckmann, L.; Lorenz, H.; Sundmacher, K. Steam reforming of glycerol: The experimental activity of La<sub>1-x</sub>Ce<sub>x</sub>NiO<sub>3</sub> catalyst in comparison to the thermodynamic reaction equilibrium. *Appl. Catal. B Environ.* **2009**, *90*, 29–37.
144. Fu, M.; Xu, Q.; Qi, W.; Zhang, Z.; Zhang, S.; Yan, Y. Hydrogen production from glycerol steam reforming over Ni/La/Co/Al<sub>2</sub>O<sub>3</sub> catalyst. *Energy Source A Recov. Utiliz. Environ. Eff.* **2016**, *38*, 2128–2134.
145. Chiodo, V.; Freni, S.; Galvagno, A.; Mondello, N.; Frusteri, F. Catalytic features of Rh and Ni supported catalysts in the steam reforming of glycerol to produce hydrogen. *Appl. Catal. A Gen.* **2010**, *381*, 1–7. [[CrossRef](#)]
146. Chen, H.; Ding, Y.; Cong, N.T.; Dou, B.; Dupont, V.; Ghadiri, M.; Williams, P.T. A comparative study on hydrogen production from steam-glycerol reforming: Thermodynamics and experimental. *Renew. Energy* **2011**, *36*, 779–788.
147. Byrd, A.J.; Pant, K.K.; Gupta, R.B. Hydrogen production from glycerol by reforming in supercritical water over Ru/Al<sub>2</sub>O<sub>3</sub> catalyst. *Fuel* **2008**, *87*, 2956–2960. [[CrossRef](#)]
148. Lin, K.H.; Lin, W.H.; Hsiao, C.H.; Chang, H.F.; Chang, A.C.C. Hydrogen production in steam reforming of glycerol by conventional and membrane reactors. *Int. J. Hydrogen Environ.* **2012**, *37*, 13770–13776. [[CrossRef](#)]
149. Wang, C.; Dou, B.; Chen, H.; Song, Y.; Xu, Y.; Du, X.; Zhang, L.; Luo, T.; Tan, C. Renewable hydrogen production from steam reforming of glycerol by Ni-Cu-Al, Ni-Cu-Mg, Ni-Mg catalysts. *Int. J. Hydrogen Environ.* **2013**, *38*, 3562–3571.
150. Iulianelli, A.; Longo, T.; Liguori, S.; Basile, A. Production of hydrogen via glycerol steam reforming in a Pd-Ag membrane reactor over Co/Al<sub>2</sub>O<sub>3</sub> catalyst. *Asia Pac. J. Chem. Eng.* **2010**, *5*, 138–145. [[CrossRef](#)]
151. Iulianelli, A.; Seelam, P.K.; Liguori, S.; Longo, T.; Keiski, R.; Calabrò, V.; Basile, A. Hydrogen production for PEM fuel cell by gas phase reforming of glycerol as byproduct of bio-diesel. The use of a Pd-Ag membrane reactor at middle reaction temperature. *Int. J. Hydrogen Environ.* **2011**, *36*, 3827–3834. [[CrossRef](#)]
152. Basile, A.; Iulianelli, A.; Bagnato, G.; Dalena, F. Hydrogen Production for PEM Fuel Cells. In *Production of Hydrogen from Renewable Resources*; Fang, Z., Smith, R.L., Qi, X., Eds.; Springer: Heidelberg, Germany, 2015; pp. 339–356.
153. Chang, A.C.-C.; Lin, W.-H.; Lin, K.-H.; Hsiao, C.-H.; Chen, H.-H.; Chang, H.-F. Reforming of glycerol for producing hydrogen in a Pd/Ag membrane reactor. *Int. J. Hydrogen Environ.* **2012**, *37*, 13110–13117. [[CrossRef](#)]
154. Lin, K.-H.; Chang, A.C.-C.; Lin, W.-H.; Chen, S.-H.; Chang, C.-Y.; Chang, H.-F. Autothermal steam reforming of glycerol for hydrogen production over packed-bed and Pd/Ag alloy membrane reactors. *Int. J. Hydrogen Environ.* **2013**, *38*, 12946–12952.
155. Silva, J.M.; Soria, M.A.; Madeira, L.M. Challenges and strategies for optimization of glycerol steam reforming process. *Renew. Sustain. Environ. Rev.* **2015**, *42*, 1187–1213. [[CrossRef](#)]
156. Davidson, S.D.; Zhang, H.; Sun, J.; Wang, Y. Supported metal catalysts for alcohol/sugar alcohol steam reforming. *Dalton Trans.* **2014**, *43*, 11782–11802. [[CrossRef](#)]
157. Dou, B.; Song, Y.; Wang, C.; Chen, H.; Xu, Y. Hydrogen production from catalytic steam reforming of biodiesel byproduct glycerol: Issues and challenges. *Renew. Sustain. Environ. Rev.* **2014**, *30*, 950–960.

158. Dal Santo, V.; Gallo, A.; Naldoni, A.; Guidotti, M.; Psaro, R. Bimetallic heterogeneous catalysts for hydrogen production. *Catal. Today* **2012**, *197*, 190–205.
159. Gallo, A.; Pirovano, C.; Ferrini, P.; Marelli, M.; Psaro, R.; Santangelo, S.; Faggio, G.; Dal Santo, V. Influence of reaction parameters on the activity of ruthenium based catalysts for glycerol steam reforming. *Appl. Catal. B Environ.* **2012**, *121–122*, 40–49. [[CrossRef](#)]
160. Bossola, F.; Evangelisti, C.; Allieta, M.; Psaro, R.; Recchia, S.; Dal Santo, V. Well-formed, size-controlled ruthenium nanoparticles active and stable for acetic acid steam reforming. *Appl. Catal. B Environ.* **2016**, *181*, 599–611.
161. Silva, J.M.; Soria, M.A.; Madeira, L.M. Thermodynamic analysis of Glycerol Steam Reforming for hydrogen production with in situ hydrogen and carbon dioxide separation. *J. Power Sources* **2015**, *273*, 423–430. [[CrossRef](#)]



© 2017 by the authors. Licensee MDPI, Basel, Switzerland. This article is an open access article distributed under the terms and conditions of the Creative Commons Attribution (CC BY) license (<http://creativecommons.org/licenses/by/4.0/>).